Journal of Sound and Vibration (1990) **139**(2) 201–225

VIBRATION TRANSMISSION THROUGH ROLLING ELEMENT BEARINGS, PART II: SYSTEM STUDIES

T. C. LIM† AND R. SINGH

Department of Mechanical Engineering, The Ohio State University, Columbus, Ohio 43210, *U.S.A.*

(*Received* 21 *June* 1989)

This paper extends the proposed bearing stiffness formulation of Part I and demonstrates its superiority over existing models in vibration transmission analyses for a generic single shaft-bearing-plate-mount system. The bearing stiffness matrix $[K]_{bm}$ is incorporated in discrete system models involving lumped parameter and finite element modeling techniques. Shaft, plate and mount flexibilities are also included in such models. The stability issue associated with the proposed bearing model is addressed analytically by using Liapunov's stability method, and the system is found to be dynamically stable provided the preloads are sufficiently high. Eigensolution and forced harmonic response to the following rolling element bearing system example cases are obtained by using our formulation and results are compared with the predictions yielded by the current vibration models: (i) rigid shaft and plate system freely suspended; (ii) rigid shaft and plate supported on flexible mounts; (iii) an experimental set-up consisting of a flexible shaft, two ball bearings, a rectangular plate and the supporting structure. Analytical results indicate that our proposed model is indeed capable of predicting plate rigid-body angular motion or plate flexural motion as excited by shaft motion. Such predictions are not observed in existing vibration models. Also, models with lower degrees of freedom, developed by several previous investigators, tend to underestimate the resonant frequencies and force or moment transmissibilities as compared with our multi-degree-of-freedom models. Finally, comparisons between our model and experiment have been found to be reasonably good.

1. INTRODUCTION

Current bearing models [1–6] cannot explain how the vibratory motion may be transmitted from the rotating shaft to the casing and other connecting structures in rotating mechanical equipment. For instance, experimental results [7–9] have shown that casing plate motion for a system similar to Figure 1 is primarily of the flexural or out-of-plane type given only the bending motion on the shaft. By using existing vibration models, only in-plane type motions on the casing plate are obtained. Such limitations associated with current bearing models have been discussed thoroughly in the companion paper, Part I [10]. Also in Part I a new mathematical model for precision rolling element bearings has been developed in order to clarify this issue qualitatively and quantitatively.

This paper extends the proposed bearing formulation and demonstrates its superiority over the existing models in vibration transmission analyses. A schematic of a generic system with a flexible shaft rotating at constant speed Ω_z, flexible casing and mount is shown in Figure 1. The shaft is supported by a rolling element bearing which is modeled by a stiffness matrix $[K]_{bm}$ of dimension six as proposed in Part I. The excitations at the rotating shaft are given in terms of an alternating load vector $\{f(t)\}_{sa} = \{F_{jsa}(t), T_{jsa}(t)\}^T = \{f(t)\}_s - \{f\}_{sm}$, $j = x, y, z$, where $F_{jsa}(t)$ and $T_{jsa}(t)$ are the alternating force and torque respectively, $\{f(t)\}_s$ is the total load vector of dimension six, $\{f\}_{sm}$ represents the mean load vector, and the superscript T implies the transpose (a list of symbols is given in the

† Presently with Structural Dynamics Research Corporation, Milford, Ohio 45150, U.S.A.

0022-460X/90/110201+25 $03.00/0

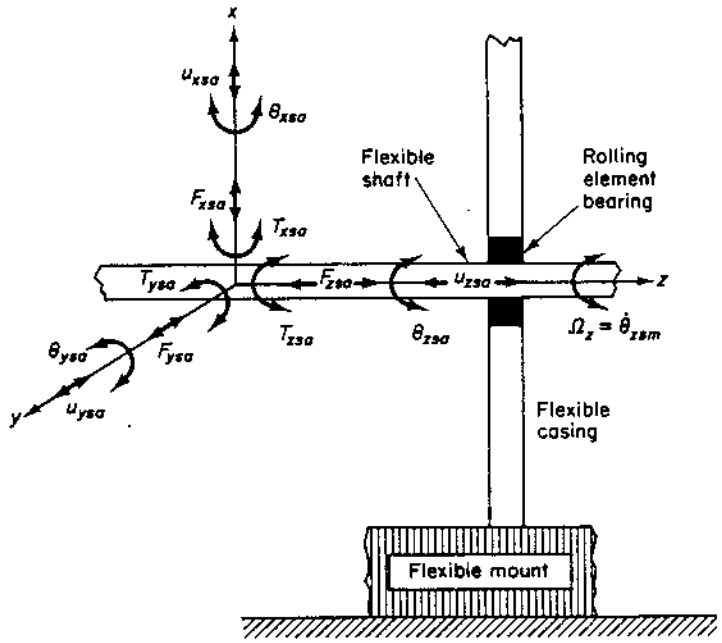

Figure 1. Schematic representation of the vibration transmission problem. Here the flexible shaft is subjected to alternating forces $F_{jsa}(t)$ and torques $T_{jsa}(t)$, where $j = x$, y or z, is the direction and subscript a implies alternating. Also, θ is the angular displacement and u is the translational displacement.

Appendix). In the vibration analysis, $\{f\}_{sm}$ and bearing preloads are not included as they do not appear in the governing equations of the linear vibration model but are used for computing $[K]_{bm}$. The effect of bearing coupling coefficients, which are off-diagonal and rotational diagonal terms of $[K]_{bm}$ as described in Part I, on the eigensolution, forced vibration and vibration transmission through bearings is evaluated. Our theory will be illustrated and validated through three physical system example cases; experimental verification is also included.

2. LITERATURE REVIEW

The existing bearing models based on assumptions of either ideal boundary conditions [1–3] for the shaft or translational stiffness elements [4–6] have already been discussed in Part I [10]. Various formulas for estimating translational stiffness coefficients commonly used by researchers have been compared with our proposed $[K]_{bm}$ formulation. These simple bearing models are widely used in vibration models of the rotor dynamic systems, which typically exclude casing and mount dynamics, to calculate critical speeds, responses due to shaft excitations such as mass unbalance and gear transmission error and dynamic stability [1–6]. In most of these cases, the vibration transmission through bearings is never or not the primary issue, and moreover such vibration models are clearly inadequate in this regard. A satisfactory study of the vibration transmission through bearings in a rotating system similar to Figure 1 is yet to be reported, even though several researchers have considered it with limited success [11–14]. In 1979 White [11] evaluated the rolling element bearing vibration transfer characteristics using a two-degrees-of-freedom (DOF) vibration model of the system shown in Figure 1. His formulation is based on only the radial bearing stiffness coefficient k_{brr}. He concluded that an increase in preload increases k_{brr} and system natural frequencies. He also found that the effect of bearing non-linearity is negligible at higher preloads. In 1987 Kraus *et al.* [14] proposed a single-degree-of-freedom model for a similar physical system (with a very compliant mount) to estimate

k_{brr} from measured vibration transmission spectra. In both of these studies, the coupling coefficients of $[K]_{bm}$ are not included.

In 1982 Rajab [12] philosophically proposed a bearing stiffness matrix which consists of k_{brr}, $k_{br\theta}$ and $k_{b\theta\theta}$ coefficients. Some of the key features of his model are also summarized in reference [13]. This model is in fact a subset of our $[K]_{bm}$ as shown in Part I [10]. Several errors in his analytical development have already been pointed out. In addition, he incorporated his bearing model in a system study using a commercial structure synthesis program [15]. However, based on our study, we have inferred that he incorrectly synthesized the system model given the plate experimental modal data, shaft finite model and analytical bearing model. Moreover, an error in this case was committed when he converted $k_{br\theta}$ and $k_{b\theta\theta}$ coefficients to "effective stiffness coefficients" which he claimed to couple the shaft bending motion to the plate out-of-plane motion. This method excludes the bearing rotational degree of freedom, which is obviously not correct.

3. ASSUMPTIONS AND OBJECTIVES

Linear discrete vibration models of the generic system shown in Figure 1 are used to incorporate $[K]_{bm}$ and to characterize the vibration transmission through rolling element bearings. The stiffness coefficients of $[K]_{bm}$ are evaluated by using the analytical expressions presented in Part I [10]. The effect of the gyroscopic moment on the shaft dynamics is not included. Since the bearing system is statically indeterminate, the direct stiffness formulation technique is used to obtain the system governing equations as opposed to the flexibility formulation. The governing equations for the system vibration model can be given in matrix form as

$$[M]\{\ddot{q}(t)\}_a+[C]\{\dot{q}(t)\}_a+[K]\{q(t)\}_a=\{f(t)\}_a, \tag{1}$$

where $[M]$, $[C]$ and $[K]$ are the system mass, damping and stiffness matrices respectively, and $\{q(t)\}_a$ and $\{f(t)\}_a$ are defined as the generalized alternating displacement and applied load vectors respectively. Due to the linearity of the vibrating system, mean shaft loads $\{f\}_{bm}$ and preloads do not directly affect the dynamic response of the rotating system and hence are excluded from equation (1). However, $\{f\}_{bm}$ and bearing preloads are assumed to be constant to ensure a time-invariant $[K]_{bm}$ matrix which depends only on these mean loads or on the mean deflection operating points. Accordingly, only the alternating shaft loads $\{f(t)\}_{sa}$ in Figure 1 which represent typical machine excitation due to the kinematic errors, mass unbalances and torque fluctuations are included in the forced vibration problem. The energy dissipation associated with the rolling element bearings is assumed to be an energy equivalent viscous damping matrix $[C]_b=\sigma[K]_{bm}$, where σ is the Rayleigh damping matrix proportionality constant. Dynamic instabilities due to the oil whirl phenomenon and asymmetry of rotating elements [2, 3] are clearly beyond the scope of this study and hence are not considered here.

The specific objectives of this study are as follows: (i) to incorporate the proposed bearing matrix $[K]_{bm}$, developed in Part I [10], in the linear discrete vibration model of the rotating mechanical equipment as described by equation (1), with use of both the lumped parameter and dynamic finite element methods; (ii) to evaluate the dynamic stability of the proposed bearing system model by using Liapunov's second method; (iii) to calculate eigensolutions and forced harmonic responses, and predict vibration transmission through rolling element bearings for three example cases; (iv) to demonstrate the advantages of our formulation over the existing models of Kraus *et al.* [14] and White [11]; (v) to validate the proposed theory by comparing analytical prediction with experimental data on an analogous system.

4. SYSTEM GOVERNING EQUATIONS

4.1. METHOD A: LUMPED PARAMETER MODEL

The proposed bearing matrix $[K]_{bm}$ can be easily implemented in equation (1). Note that the coupling coefficients of $[K]_{bm}$ provide the capability to predict casing rigid-body angular $\theta_{jca}(t)$, $j = x, y, z$, and translational $u_{jca}(t)$ motions, given only the unidirectional transverse shaft forces. Hence one can couple the shaft motions to the motions of a casing of a system similar to Figure 1 but with a rigid shaft and a rigid casing using a lumped parameter model. The bearing preloads can now be included in the mean shaft load vector $\{f\}_{bm}$ by a direct vector addition, as the rigid shaft can be assumed to be a single lumped mass for this purpose. An alternating displacement vector $\{q(t)\}_a = \{\{q(t)\}_{sa}^T, \{q(t)\}_{ca}^T\}^T$, is defined, where $\{q(t)\}_{sa} = \{u_{jsa}(t), \theta_{jsa}(t)\}^T$ and $\{q(t)\}_{ca} = \{u_{jca}(t), \theta_{jca}(t)\}^T$, $j = x, y, z$, are the shaft and casing alternating displacement vectors respectively. The governing equations of motion for this generic vibration model with 12 degrees of freedom are given by equation (1) with

$$[M] = \begin{bmatrix} [M]_s & [0] \\ [0] & [M]_c \end{bmatrix}, \qquad [K] = \begin{bmatrix} [K]_{bm} & -[K]_{bm} \\ -[K]_{bm} & [K]_{bm} + [K]_v \end{bmatrix}, \tag{2a, b}$$

$$[C] = \sigma[K], \qquad \{f(t)\}_a = \begin{Bmatrix} \{f(t)\}_{sa} \\ \{0\} \end{Bmatrix}, \tag{2c, d}$$

$$[K]_{bm} = \begin{bmatrix} k_{bxx} & k_{bxy} & k_{bxz} & k_{bx\theta_x} & k_{bx\theta_y} & 0 \\ & k_{byy} & k_{byz} & k_{by\theta_x} & k_{by\theta_y} & 0 \\ & & k_{bzz} & k_{bz\theta_x} & k_{bz\theta_y} & 0 \\ & & & k_{b\theta_x\theta_x} & k_{b\theta_x\theta_y} & 0 \\ & \text{symmetric} & & & k_{b\theta_y\theta_y} & 0 \\ & & & & & 0 \end{bmatrix}, \tag{2e}$$

where the stiffness matrices $[K]_{bm}$ and $[K]_v$ pertain to the bearing and mount respectively, and the matrices $[M]_s$ and $[M]_c$ are diagonal shaft and casing mass matrices respectively; each matrix of dimension six. Specific examples of this method along with the eigensolution and forced response studies will be presented in sections 7 and 8.

4.2. METHOD B: DYNAMIC FINITE ELEMENT FORMULATION

Consider the dynamic finite element method of incorporating $[K]_{bm}$ in equation (1) especially when the shaft and casing plate are elastically deformable over the frequency range of interest. This method is different from the lumped parameter formulation of section 4.1, for which a non-compliant shaft and casing were assumed. For example, if the flexible casing plate is considered to be very large compared to the bearing dimensions, then the bearing nodal point on the shaft can be coupled to only one bearing nodal point on the plate as shown in Figure 2(a). Accordingly, the present form of $[K]_{bm}$ is implemented in the finite element model as a generalized stiffness matrix like the lumped parameter model. On the other hand, when the flexible casing plate dimensions are finite and of the order of bearing dimensions, then several bearing nodal points are considered as shown in Figure 2(b). In the discretization philosophy here it is assumed that a relative displacement vector, given by the difference between the averaged displacement vector of bearing nodal points on the plate and the displacement vector of a bearing nodal point on the shaft, is equivalent to the actual rigid-body bearing motion. Accordingly, we divide the bearing stiffness coefficients equally among all the generalized stiffness elements connecting the bearing nodal points on the plate to a single bearing nodal point on the

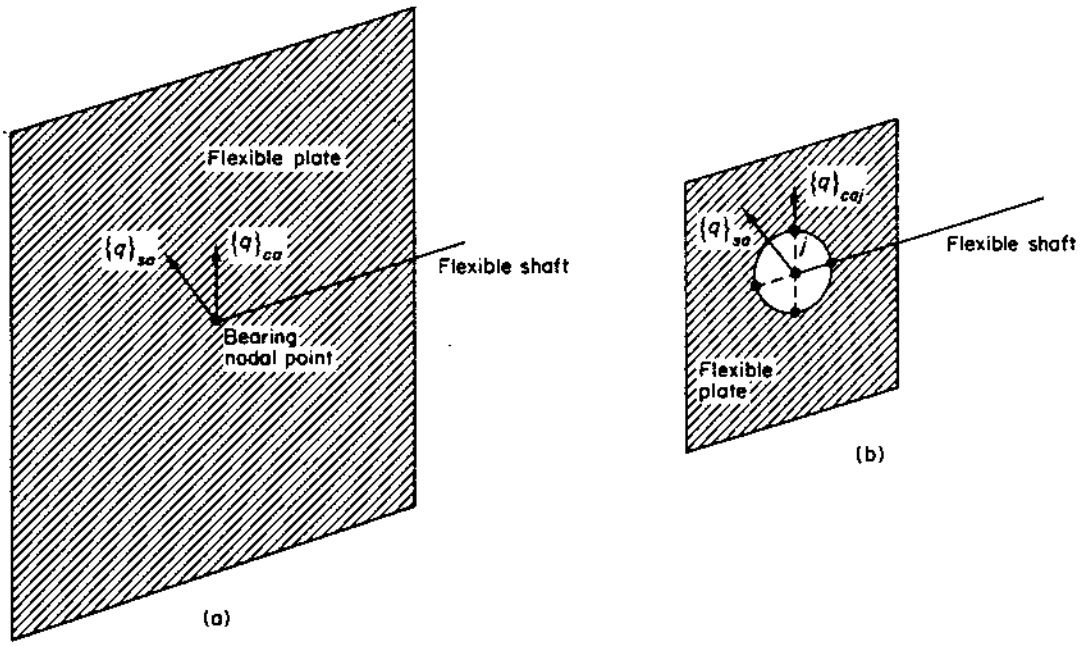

Figure 2. Discretization method for implementation of $[K]_{bm}$ in finite element model of a system similar to Figure 1. Here $\{q(t)\}_{sa}$ and $\{q(t)\}_{ca}$ are the alternating shaft and plate displacement component. (a) Single bearing nodal point on the plate; (b) multiple bearing nodal points on the plate.

shaft. In the limit, where all the bearing nodal points on the plate are collapsed to a single nodal point, $[K]_{bm}$ is recovered as in the first method. Our finite element formulation uses conventional structural elements typically available in commercial software programs [16]—this will be illustrated in section 9. Other features of this method are similar to those discussed earlier in section 4.1.

4.3. OTHER METHODS

Alternate methods of incorporating $[K]_{bm}$ in equation (1) such as the finite difference method which is similar to method B, flexibility, component mode synthesis and transfer matrix formulations are also possible. In the flexibility formulation, the bearing flexibility matrix can be obtained by inverting a subset of the bearing stiffness matrix $[K]_{bms}$ which excludes zeroes corresponding to the θ_z angular direction from $[K]_{bm}$. In the transfer matrix method, the field matrix $[T]_b$ for a bearing can be easily related to $[K]_{bms}$.

$$\begin{Bmatrix} \{q(t)\}_{sa} \\ \{f(t)\}_{sa} \end{Bmatrix} = [T]_b \begin{Bmatrix} \{q(t)_{ca} \\ \{f(t)\}_{ca} \end{Bmatrix}, \qquad [T]_b = \begin{bmatrix} [I] & [K]_{bms}^{-1} \\ [0] & [I] \end{bmatrix}, \tag{3a, b}$$

where $\{\{q(t)\}_{sa}^{\mathrm{T}}, \{f(t)\}_{sa}^{\mathrm{T}}\}^{\mathrm{T}}$ and $\{\{q(t)\}_{ca}^{\mathrm{T}}, \{f(t)\}_{ca}^{\mathrm{T}}\}^{\mathrm{T}}$ are now the state vectors at bearing locations on the shaft and casing plate respectively. Equation (3) can now be integrated with transfer matrices of the shaft and plate which are well documented in references [17, 18]. Direct application of these alternate methods [17–20] are beyond the scope of this paper and are left for further research.

5. BEARING SYSTEM STABILITY

The stability of the proposed linear, non-gyroscopic model of a bearing system similar to Figure 1, which is governed by equation (1) with $\{f(t)\}_a = \{0\}$, can be determined by using several techniques such as Liapunov's stability method, or the Routh-Hurwitz criteria, or from the direct evaluation of system eigenvalues. Here Liapunov's second

method is used for its simplicity when applid to such a vibration model [21, 22]. If the system matrices $[M]$, $[C]$ and $[K]$ of equation (1) are always symmetric and positive definite, then the system is asymptotically stable per Liapunov. The first condition is directly satisfied since $[M]$, $[C]$ and $[K]$ are symmetric. Further, since $[M]$ is diagonal and consists of only positive entries, it is clearly positive definite. For $[K]$, the positive definite test can be performed by evaluating its principal minor determinants, which is demonstrated here for the generic lumped parameter model. Consider the decomposition of $[K]$ given by equation (2) into a product of three matrices,

$$[K]=\begin{bmatrix} [I] & [0] \\ -[I] & [I] \end{bmatrix}\begin{bmatrix} [K]_{bm} & [0] \\ [0] & [K]_v \end{bmatrix}\begin{bmatrix} [I] & -[I] \\ [0] & [I] \end{bmatrix}, \tag{4}$$

where the square submatrix [0] of the appropriate dimension consists of only zero entries, $[I]$ is an identity matrix of the same dimension, and $[K]_{bm}$ and $[K]_v$ have been defined in section 4.1. The determinant of $[K]$ is the product of the determinants of the three matrices on the right side of equation (4),

$$|K|=|[K]_v||[K]_{bm}|. \tag{5}$$

If $|[K]_{wj}|>0$, $w, j=1,2,\ldots,P$ and $P=1,2,\ldots,12$, $[K]$ is positive definite. The other principal minor determinant with $P<12$ can be obtained by excluding the stiffness coefficients which are not entries in the principal submatrix of equation (5). Since $|[K_v]|=k_{vx}\cdot k_{vy}\cdot k_{vz}\cdot k_{v\theta_x}\cdot k_{v\theta_y}\cdot k_{v\theta_z}>0$, it implies that equation (5) is positive only if $|[K]_{bm}|$ is positive. One may recall that $[K]_{bm}$ has zero entries in the last row and in the last column corresponding to the torsional θ_z angular direction which forces the bearing system to be semidefinite. Now define a new matrix $[K]_{bms}$ of dimension five as a subset of $[K]_{bm}$ with these zeroes excluded. If $[K]_{bms}$ has positive principal minor determinants, then this system is dynamically stable because it will consist of stable oscillations superimposed on the mean shaft rotational motion $\Omega_z\neq\Omega_z(t)$. Further, it follows that $[C]_{bms}$, which is proportional to $[K]_{bms}$, is also positive definite if $[K]_{bms}$ is positive definite. The resulting equation obtained from the expansion of the determinant of $[K]_{bms}$ in terms of its entries k_{bwj}, $w, j=1,2,3,4,5$, is given as follows in terms of the stability functions $\Phi_j, j=1,2,3,4$:

$$\begin{aligned}
|[K]_{bms}| &= 2\Phi_4(55,34,45,35)\{k_{b24}\Phi_4(11,23,12,13)+k_{b14}\Phi_4(22,13,12,23)\}\\
&\quad +2\Phi_4(44,35,45,34)\{k_{b25}\Phi_4(11,23,12,13)+k_{b15}\Phi_4(22,13,12,23)\}\\
&\quad +2\Phi_4(24,35,25,34)\{k_{b14}\Phi_4(25,13,23,35)+k_{b15}\Phi_4(12,34,24,13)\}\\
&\quad -k_{b15}k_{b22}k_{b34}\Phi_3(14,35,15,34)+k_{b24}k_{b15}k_{b14}\Phi_3(23,35,33,25)\\
&\quad +2k_{b14}\Phi_4(25,45,24,55)\Phi_4(13,23,12,33)+\{k_{b14}k_{b25}\}^2k_{b33}\\
&\quad +\Phi_1(1,2)\Phi_2(45,34,35,44,55)+\Phi_1(1,3)\Phi_2(45,24,25,44,55)\\
&\quad +k_{b15}\Phi_1(2,3)\Phi_3(14,45,15,44)+k_{b11}\{\Phi_4(24,35,25,34)\}^2\\
&\quad +\{k_{b14}\}^2\{k_{b23}\Phi_3(23,55,35,25)-k_{b22}\Phi_1(3,5)\}\\
&\quad +\Phi_1(4,5)\{k_{b11}\Phi_1(2,3)+\Phi_2(23,13,12,33,22)\}\\
&\quad +2k_{b15}\Phi_4(24,45,25,44)\Phi_4(23,13,12,33)\\
&\quad +2k_{b15}\Phi_4(14,25,15,24)\Phi_4(23,34,24,33),
\end{aligned} \tag{6a}$$

$$\Phi_1(w_I,w_{II})=k_{bw_Iw_I}k_{bw_{II}w_{II}}-\{k_{bw_Iw_{II}}\}^2, \tag{6b}$$

$$\Phi_2(w_I,w_{II},w_{III},w_{IV},w_V)=2k_{bw_I}k_{bw_{II}}k_{bw_{III}}-k_{bw_{IV}}\{k_{bw_{III}}\}^2-k_{bw_V}\{k_{bw_{II}}\}^2, \tag{6c}$$

TABLE 1

Bearing system stability criteria for the proposed ball bearing model; $j = x$ *or* 1, y *or* 2; $p = x$ *or* 1, y *or* 2 *but* $p \neq j$

Proposed bearing model† (see Table 2 in reference [10])	Stability criteria‡
$k_{xx}, k_{yy}, k_{zz}, k_{\theta_x\theta_x}, k_{\theta_y\theta_y}, k_{z\theta_p}$	$\Phi_1(3, p+3) > 0$
$k_{xx}, k_{yy}, k_{zz}, k_{\theta_x\theta_x}, k_{\theta_y\theta_y}, k_{x\theta_y}, k_{y\theta_x}$	$\Phi_1(1, 5) > 0;\ \Phi_1(2, 4) > 0$
$k_{xx}, k_{yy}, k_{zz}, k_{\theta_x\theta_x}, k_{\theta_y\theta_y}$	Always stable
$k_{xx}, k_{yy}, k_{zz}, k_{\theta_x\theta_x}, l_{\theta_y\theta_y}, k_{pz}$	$\Phi_1(p, 3) > 0$
$k_{xx}, k_{yy}, k_{zz}, k_{\theta_x\theta_x}, k_{\theta_y\theta_y}, k_{xy}, k_{\theta_x\theta_y}, k_{z\theta_x}, k_{z\theta_y}$	$\Phi_1(1, 2) > 0;\ \Phi_1(3, 4) > 0;$ $k_{33}\Phi_1(4, 5) + \Phi_2(4\,5, 3\,4, 3\,5, 4\,4, 5\,5) > 0$
$k_{xx}, k_{yy}, k_{zz}, k_{\theta_x\theta_x}, k_{\theta_y\theta_y}, k_{x\theta_y}, k_{y\theta_x}, k_{jz}, k_{z\theta_p}$	$k_{11}k_{22}\Phi_1(3, 4) + k_{j3}^2 k_{pp}k_{44} + k_{14}^2 k_{22}k_{33} > 0;$ $\Phi_1(j, 3) > 0;$ $\{k_{33}\Phi_1(1, 4)\Phi_1(2, 5)\Phi_5(p\,p+3, j+3j+3, p\,p, 4\,4, 5\,5)\}$ $\cdot \{k_{j3}k_{3\,p+3}\}^2 \cdot \{\Phi_5(j\,j+3, p\,p, 1\,1, 2\,2, j+3\,j+3)\} > 0$
$k_{xx}, k_{yy}, k_{zz}, k_{\theta_x\theta_x}, k_{\theta_y\theta_y}, k_{xy}, k_{xz}, k_{yz}, k_{\theta_x\theta_y}$	$\Phi_1(4, 5) > 0;\ \Phi_1(1, 2) > 0;$ $k_{11}\Phi_1(1, 2) + \Phi_2(2\,3, 1\,2, 1\,3, 2\,2, 3\,3) > 0$
$k_{xx}, k_{yy}, k_{zz}, k_{\theta_x\theta_x}, k_{\theta_y\theta_y}, k_{x\theta_x}, k_{y\theta_x}, k_{jz}, k_{z\theta_p}$	$\Phi_1(p, j+3) > 0;\ \Phi_1(j, 3) > 0;$ $k_{jj}\Phi_1(3, p+3) + \Phi_2(3p+3, j\,3, j\,p+3, 3\,3, p+3\,p+3) > 0$
All non-zero except θ_z terms	$\lvert[K]_{bms}\rvert > 0$

† Here the subscript b which implies bearing has been omitted for brevity.
‡ Stability functions Φ_1 and Φ_2 are defined by equations (6b) and (6c) and Φ_5 is given by $\Phi_5(w_I, w_{II}, w_{III}, w_{IV}, w_V) = \{k_{bw_I}\}^2 k_{bw_{II}} - k_{bw_{III}}k_{bw_{IV}}k_{bw_V}$.

TABLE 2

Bearing system stability criteria for the proposed roller bearing model; $j = x$ *or* 1, y *or* 2; $p = x$ *or* 1, y *or* 2 *but* $p \neq j$

Proposed bearing model† (see Table 3 in reference [10])	Stability criteria‡
k_{jj}	Always stable
$k_{xx}, k_{yy}, k_{zz}, k_{\theta_x\theta_x}, k_{\theta_y\theta_y}, k_{x\theta_y}, k_{y\theta_x}$	$\Phi_1(1, 5) > 0;\ \Phi_1(2, 4) > 0$
$k_{zz}, k_{\theta_x\theta_x}, k_{\theta_y\theta_y}$	Always stable
$k_{zz}, k_{\theta_x\theta_x}, k_{\theta_y\theta_y}, k_{z\theta_j}$	$\Phi_1(3, j+3) > 0$
k_{xx}, k_{yy}, k_{xy}	$\Phi_1(1, 2) > 0$
$l_{xx}, k_{yy}, k_{zz}, k_{\theta_x\theta_x}, k_{\theta_y\theta_y}, k_{x\theta_y}, k_{y\theta_x}, k_{jz}, k_{z\theta_p}$	$\Phi_1(p, j+3) > 0;\ \Phi_1(j, 3) > 0;$ $k_{jj}\Phi_1(3, p+3) + \Phi_2(3\,p+3, j3, j\,p+3, 3\,3, p+3\,p+3) > 0$
$k_{zz}, k_{\theta_x\theta_x}, k_{\theta_y\theta_y}, k_{\theta_x\theta_y}, k_{z\theta_x}, k_{z\theta_y}$	$\Phi_1(3, 4) > 0;$ $k_{33}\Phi_1(4, 5) + \Phi_2(4\,5, 3\,4, 3\,5, 4\,4, 5\,5) > 0$
All non-zero except θ_z terms	$\lvert[K]_{bms}\rvert > 0$

† Here the subscript b which implies bearing has been omitted for brevity.
‡ Functions Φ_1 and Φ_2 are defined by equations (6b) and (6c).

$$\Phi_3(w_I, w_{II}, w_{III}, w_{IV}) = 2k_{bw_I}k_{bw_{II}} - k_{bw_{III}}k_{bw_{IV}}, \tag{6d}$$

$$\Phi_4(w_I, w_{II}, w_{III}, w_{IV}) = k_{bw_I}k_{bw_{II}} - k_{bw_{III}}k_{bw_{IV}}, \tag{6e}$$

where $w_j, j = I, II, III, IV, V$, are the dummy variables and each w_j may represent either a single number or a set of two numbers in equation (6a). The principal minor determinants of $[K]_{bms}$ can also be derived from equation (6) by excluding the appropriate stiffness coefficients which are not entries of the particular principal submatrix. Hence, the bearing system is stable if each principal minor determinant derived from equation (6) is positive. The stability of the proposed bearing model given in Part I [10] can now be verified by using these conditions. Inequalities associated with the stability criteria for these models are summarized in Tables 1 and 2 for ball and roller bearings respectively. These inequalities arise due to the fact that we are yet to impose any restrictions on these

TABLE 3

Design parameters for typical ball and roller bearings used for system studies

Parameters	Ball type	Roller type
Load-deflection exponent n	3/2	10/9
Load-deflection constant, K_n(N/m^n)	1·0E9	1·0E8
Number of rolling elements, Z	12	14
Radial clearance, r_L (mm)	0·00005	0·00175
Pitch diameter (mm)	40·05	38·00
A_0 (mm)†	0·05	—
Unloaded contact angle, α_0	40°	15°

† Unloaded distance between inner and outer raceway groove curvature centers.

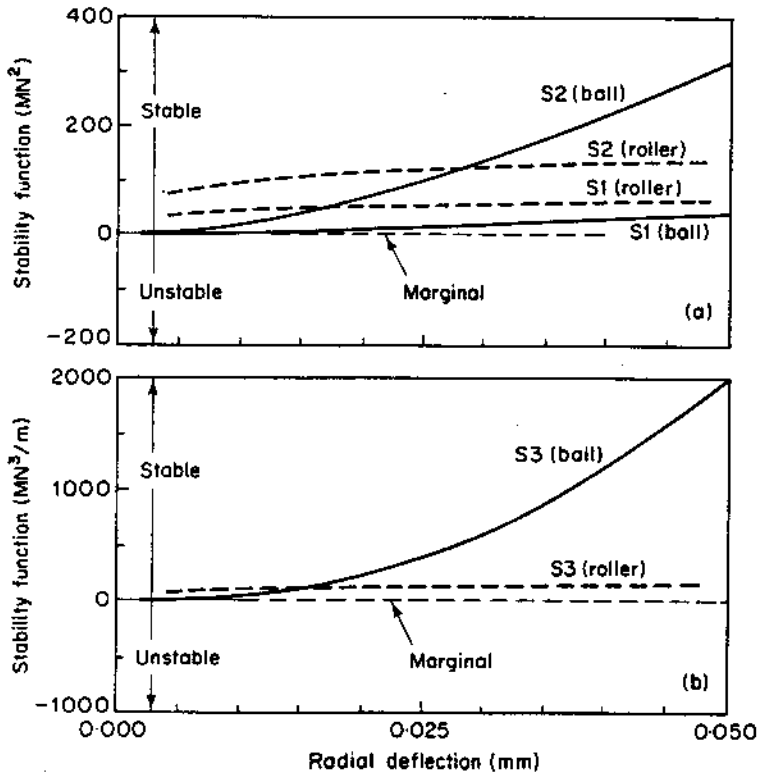

Figure 3. Plot of stability criteria functions for ball and roller bearings subjected to mean bearing radial deflection δ_{xm}. (a) S1 = $\Phi_1(2, 4)$ and S2 = $\Phi_1(1, 3)$; (b) S3 = $k_{b11}\Phi_1(3, 5) + \Phi_2(35, 13, 15, 33, 44)$.

stiffness coefficients. In Part I, these stiffness coefficients were given as functions of bearing kinematic and design parameters, and hence any coefficient cannot assume an arbitrary value as it is related uniquely to other coefficients through these parameters. Extensive numerical studies performed over a wide range of these parameters have indicated that the bearing models proposed in Part I are indeed stable provided that the preloads are sufficiently large to avoid the clearance non-linearity. Examples of these bearing system stability studies for precision rolling element bearings, the design data for which are given in Table 3, are illustrated in Figures 3–5. In all of these figures, the stability functions Φ_j given in Tables 1 and 2 are found to lie within the stable region.

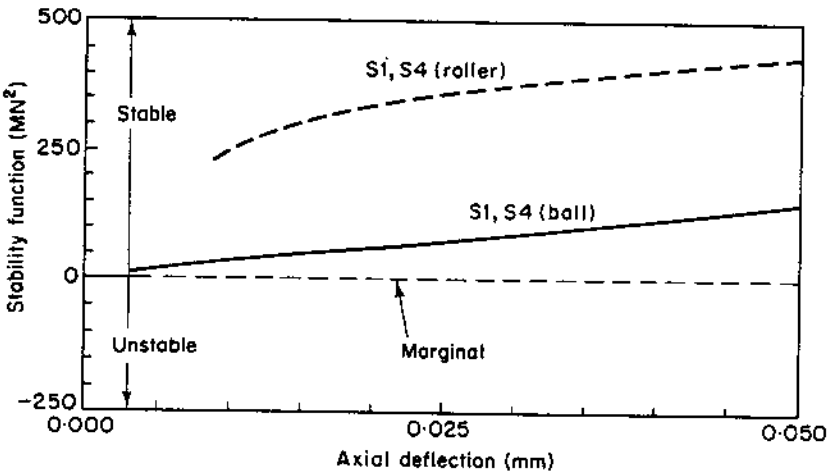

Figure 4. Plot of stability criteria functions for ball and roller bearings subjected to mean bearing axial deflection δ_{zm}. Here, S1 = $\Phi_1(2, 4)$ and S4 = $\Phi_1(1, 5)$.

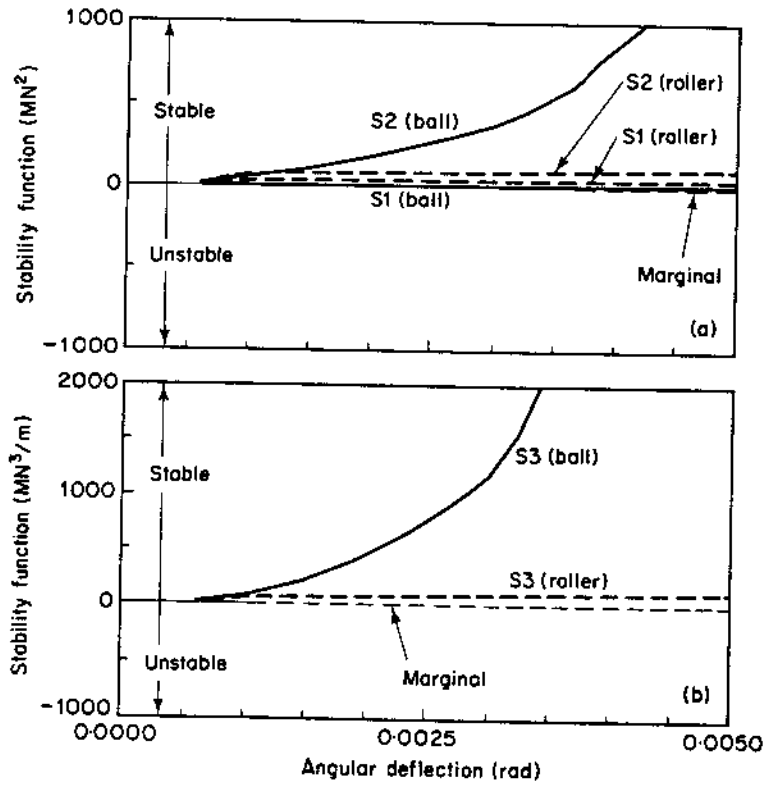

Figure 5. Plot of stability criteria functions for ball and roller bearings subjected to mean angular misalignment β_{ym}. (a) S1 = $\Phi_1(2, 4)$ and S2 = $\Phi_1(1, 3)$; (b) S3 = $k_{b11}\Phi_1(3, 5) + \Phi_2(35, 13, 15, 33, 44)$.

6. SYSTEM RESPONSE

The eigensolution of the linear, non-gyroscopic undamped system, formulated by setting $\{f(t)\}_a = \{0\}$ and $[C] = [0]$ in equation (1) given by method A or B, yields real valued natural frequencies ω_j, $j = 1, 2, 3, \ldots$, and the modal matrix $[U] = [\{\phi\}_1, \{\phi\}_2, \ldots, \{\phi\}_j, \ldots]$ for the stable system. Since the system is proportionally damped, the modal damping ratio is $\zeta_j = \sigma\omega_j^2/2$ and the damped natural frequency is given by $\omega_{jd} = \omega_j\sqrt{1-\zeta_j^2}$. Free vibration response due to the initial conditions is not considered as only the steady state particular solution corresponding to a sinusoidal or periodic load vector $\{f(t)\}_a$ is of primary interest. The excitation is defined by the Fourier series expansion $\{f(t)\}_a = \sum_p \{f\}_{ap} e^{i\omega_p t}$, where $\omega_p = p\omega_0$, ω_0 is the fundamental frequency, and $\{f\}_{ap}$ is the complex Fourier coefficient load vector. The steady state particular solution $\{q(t)\}_a$ is given by the normal mode expansion technique [17, 19, 20] as

$$\{q(t)\}_a = [U]\left(\sum_p \{\mu\}_p e^{i\omega_p t}\right), \quad \mu_{jp} = \frac{\{\phi\}_j^T\{f\}_{ap}}{\omega_j^2 - \omega_p^2 + i2\zeta_j\omega_j\omega_p}, \qquad p = 1, 2, \ldots, \quad (7a, b)$$

An alternative approach would be to assume a harmonic solution for the alternating displacement, $\{q(t)\}_a = \sum_p \{q\}_{ap} e^{i\omega_p t}$. Substituting this and the definition of $\{f(t)\}_a$ into equation (1) gives

$$\{q\}_{ap} = \frac{\text{Adj}\,[-\omega_p^2[M] + \lambda[K]]}{|[-\omega_p^2[M] + \lambda[K]|}\{f\}_{ap}, \qquad \lambda = 1 + i\sigma\omega_p, \qquad (8a, b)$$

where the operator Adj refers to the adjoint of the dynamic stiffness matrix. Features of this method are summarized in references [17, 19, 20]. Since the vibration transmission across the bearing is the primary issue, one can now define sinusoidal load transmissibility $R(p\omega)$ terms between two arbitrary locations I and II as

$$R_{f_{wIa}, f_{jIIa}}(\omega_p) = \frac{|f_{wIa}(\omega_p)|}{|f_{jIIa}(\omega_p)|}, \qquad w, j = 1, 2, \ldots, 6, \qquad (9)$$

where f_{wIa} and f_{jIIa} are components of the dynamic load vectors at two arbitrary locations I and II respectively. The accelerance $A(\omega_p)$ and mobility $V(\omega_p)$ transfer functions with motion at location I due to an alternating force or torque f_{jIIa} applied at location II on the shaft are

$$A_{q_{wIa}, f_{jIIa}}(\omega_p) = \frac{|\ddot{q}_{wIa}(\omega_p)}{|f_{IIa}(\omega_p)|}, \quad V(\omega_p) = \frac{1}{i\omega_p}A(\omega_p), \qquad w, j = 1, 2, \ldots, 6, \quad (10a, b)$$

where $\ddot{q}_{wIa}$ is a component of the acceleration vector at location I. Other frequency response functions can also be defined in a similar manner [17, 19, 20].

7. EXAMPLE CASE I: RIGID SHAFT AND PLATE SYSTEM

7.1. VIBRATION MODELS

Consider the mechanical system shown in Figure 6(a), which is assumed to be freely suspended or softly mounted such that $[K]_v \approx [0]$. A ball bearings (see Table 3) with constant axial preload is supporting a short rigid shaft subjected to a mean torque $T_{zsm} \neq T_{zsm}(t)$ and a sinusoidal radial force $F_{rsa}(t) = F_{rsa1} e^{i\omega_0 t}$ applied very close to the bearing. A lumped parameter model with 12 degrees of freedom is proposed in Figure 6(b). Conversely, the same system has also been analyzed by Kraus *et al.* [14] using a simple vibration model with one degree of freedom as shown in Figure 6(c), with only

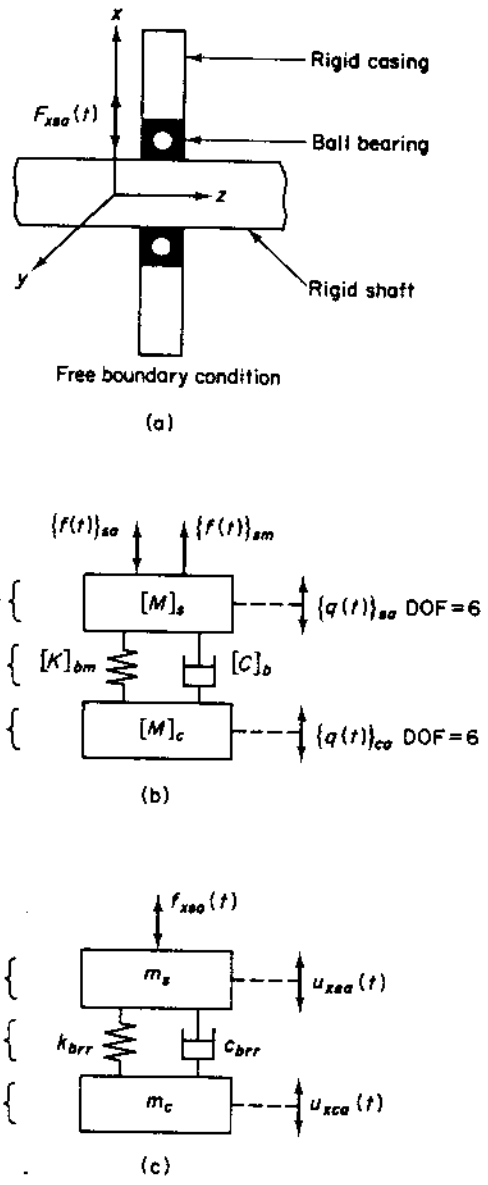

Figure 6. Example case I: freely suspended rigid shaft, ball bearing and rigid plate system subjected to alternating radial force $F_{rsa}(t)$ applied at the shaft. (a) Physical system; (b) proposed multi-degree-of-freedom vibration model with DOF = 12; (c) simple model of Kraus *et al.* [14] with DOF = 1.

the k_{brr} coefficient. The bearing stiffness matrix for an axially preloaded ball bearing in Figure 6(b) has non-negligible stiffness coefficients k_{bxx}, k_{byy}, k_{bzz}, $k_{b\theta_x\theta_x}$, $k_{b\theta_y\theta_y}$, $k_{bx\theta_y}$ and $k_{by\theta_x}$, which are functions of the mean axial preload as given in Part I [10]. The system matrices of equation (2) can be modified for this case by suppressing other bearing stiffness coefficients and $[K]_v$. It can be easily observed from equations (1) and (2) that five sets of uncoupled differential equations exist. The simplest three sets are homogeneous and pertain to the rigid body torsional motions $\theta_{za}(t)$ of the shaft and casing, and axial vibration $u_{za}(t)$ of the shaft-casing system, which are of no interest here. The remaining two sets are almost identical and associated with either $\{u_{xa}(t), \theta_{ya}(t)\}^T$ or $\{u_{ya}(t), \theta_{xa}(t)\}^T$ degrees of freedom for the rigid shaft and casing. If the co-ordinate system is chosen such that the $F_{rsa}(t)$ line of action coincides with the x-axis, then the steady state solution to the set of differential equations in terms of $\{u_{ya}(t), \theta_{xa}(t)\}^T$ is trivial. Hence, the problem reduces to a semi-definite vibration system with four degrees of freedom. Accordingly, one can rewrite $[M]_s$, $[M]_c$ and $[K]_{bm}$ in equation (2) in terms of the displacement

vector $\{q(t)\}_a = \{u_{xsa}(t), \theta_{ysa}(t), u_{xca}(t), \theta_{yca}(t)\}^T$ as

$$[M]_s = \begin{bmatrix} m_s & 0 \\ 0 & I_s \end{bmatrix}, \qquad [M]_c = \begin{bmatrix} m_c & 0 \\ 0 & I_c \end{bmatrix}, \qquad [K]_{bm} = \begin{bmatrix} k_{bxx} & k_{bx\theta_y} \\ k_{bx\theta_y} & k_{b\theta_y\theta_y} \end{bmatrix}. \quad (11a\text{–}c)$$

The first two eigenvalues corresponding to the rigid body motions in the x and θ_y directions are zero. The dimension of equation (11) is further reduced to two by defining relative motions $\delta_{xa}(t) = u_{xsa}(t) - u_{xca}(t)$ and $\beta_{ya}(t) = \theta_{ysa}(t) - \theta_{yca}(t)$, which turn out to be the bearing rigid-body motions:

$$\begin{bmatrix} \gamma_m m_s & 0 \\ 0 & \gamma_I I_s \end{bmatrix} \begin{Bmatrix} \ddot{\delta}_{xa} \\ \ddot{\beta}_{ya} \end{Bmatrix} + [C] \begin{Bmatrix} \dot{\delta}_{xa} \\ \dot{\beta}_{ya} \end{Bmatrix} + [K]_{bm} \begin{Bmatrix} \delta_{xa} \\ \beta_{ya} \end{Bmatrix} = \begin{Bmatrix} \gamma_m F_{xsa}(t) \\ 0 \end{Bmatrix}, \quad (12a)$$

$$\gamma_m = m_c/(m_s + m_c), \qquad \gamma_I = I_c/(I_s + I_c), \qquad [C] = \sigma[K]_{bm}. \quad (12b\text{–}d)$$

It may be noted that the purely translational $\delta_{xa}(t)$ model of Kraus *et al.* [14] shown in Figure 6(c) constitutes a subset of equation (12) with $k_{bx\theta_y} = 0$. Eigensolution of equation (12) with $[C] = [0]$ yields the following natural frequencies ω_j and modes $\{\phi\}_j$:

$$\omega_{1,2} = \sqrt{(B_1 \pm B_2)/2\gamma_m m_s \gamma_I I_s}, \qquad B_1 = \gamma_m m_s k_{b\theta_y\theta_y} + \gamma_I I_s k_{bxx}, \quad (13a, b)$$

$$B_2 = \sqrt{(\gamma_m m_s k_{b\theta_y\theta_y} - \gamma_I I_s k_{bxx})^2 + 4\gamma_m m_s \gamma_I I_s k_{bx\theta_y}^2}, \quad (13c)$$

$$\{\phi\}_{1,2}^T = \frac{1}{\sqrt{\gamma_m m_s + \gamma_I I_s B_3^2}} \{1, B_3\}, \qquad B_3 = \frac{\gamma_m m_s k_{b\theta_y\theta_y} - \gamma_I I_s k_{bxx} \pm B_2}{2\gamma_I k_{bx\theta_y}}. \quad (14a, b)$$

On the other hand, the eigensolution of the single degree of freedom system is given by $\hat{\omega}_2 = \sqrt{k_{bxx}/\gamma_m m_s}$ and $\{\hat{\phi}\}_1^T = \{1/\sqrt{\gamma_m m_s}\}$, where the subscript 2 and superscript $\hat{}$ are chosen to indicate that this solution essentially estimates ω_2 and $\{\phi\}_2$ in equations (13) and (14). Since $\hat{\omega}_2$ does not include $k_{bx\theta_y}$ and $k_{b\theta_y\theta_y}$, $\hat{\omega}_2 < \omega_2$, as is evident from Table 4 for three different axial preloads. This natural mode is dominated by $\delta_{xa}(t)$ as indicated by equation (14). The first mode $\{\phi\}_1$, which is predominantly $\beta_{ya}(t)$, is also affected by the axial preload.

7.2. BEARING TRANSMISSIBILITY

The forced harmonic response of equation (12) can be obtained by using the dynamic stiffness approach of equation (8):

$$\delta_{xa}(t) = \frac{(k_{b\theta_y\theta_y}\lambda - \omega_0^2 \gamma_I I_s)\gamma_m F_{xsa1} e^{i\omega_0 t}}{(k_{b\theta_y\theta_y}\lambda - \omega_0^2 \gamma_I I_s)(k_{bxx}\lambda - \omega_0^2 \gamma_m m_s) - (k_{bx\theta_y}\lambda)^2}, \quad (15a)$$

$$\beta_{ya}(t) = \frac{-k_{bx\theta_y}\lambda \gamma_m F_{xsa1} e^{i\omega_0 t}}{(k_{b\theta_y\theta_y}\lambda - \omega_0^2 \gamma_I I_s)(k_{bxx}\lambda - \omega_0^2 \gamma_m m_s) - (k_{bx\theta_y}\lambda)^2}. \quad (15b)$$

TABLE 4

Bearing stiffness coefficients and undamped natural frequencies (Hz) *of example case* I†

Axial preload F_{zbm} (N)	Bearing stiffness coefficients			Proposed model (DOF = 2)		Simple model (DOF = 1)
	k_{bxx} (N/m)	$k_{bx\theta_y}$ (N)	$k_{b\theta_y\theta_y}$ (Nm)	ω_1	ω_2	$\hat{\omega}_2$
115	1·84E7	−3·05E6	1·36E4	156	372	341
190	2·13E7	−3·12E6	1·70E5	191	395	367
285	2·43E7	−3·09E6	2·02E5	221	416	392

† Other system parameters are $m_s = 10{\cdot}0$ kg, $I_s = 0{\cdot}025$ kgm^2, $\gamma_m = 0{\cdot}4$, $\gamma_s = 0{\cdot}3$, $\sigma = 1$E-6 s.

It can be seen from equation (15) that $F_{xsa}(t)$ not only excites $\delta_{xa}(t)$ but $\beta_{ya}(t)$ as well, which is obviously not predicted by Kraus *et al.* [14]. The steady state solution for this simple model is given by the following (compare it with equation (15a)):

$$\hat{\delta}_{xa}(t) = \gamma_m F_{xsa1}\, e^{i\omega_0 t}/(k_{bxx}\lambda - \omega_0^2 \gamma_m m_s). \tag{16}$$

Both models are used to determine the load transmissibility magnitude terms $R(\omega_0)$ which are computed by using $\{\delta_{xa}(t), \beta_{ya}(t)\}^T$, $[K]$ and $[C]$. The dynamic bearing force $F_{xba}(t)$ and moment $M_{yba}(t)$ magnitudes excited by the shaft force $F_{xsa}(t)$ are given by the force transmissibility $R_{F_{xba},F_{xsa}}(\omega_0)$ and moment transmissibility $R_{M_{bya},F_{xsa}}(\omega_0)$ respectively:

$$R_{F_{xba},F_{xsa}}(\omega_0) = \frac{\gamma_m \sqrt{(1+\sigma^2\omega_0^2)B_4 + (1+\sigma^2\omega_0^2)B_5}}{\sqrt{(1+\sigma^2\omega_0^2)^2 B_4 + (1+\sigma^2\omega_0^2)(B_5+B_6)+B_7}}, \tag{17a}$$

$$R_{M_{yba},F_{xsa}}(\omega_0) = \frac{\gamma_m \gamma_I I_s \omega_0^2 \sqrt{(1+\sigma^2\omega_0^2)k_{bx\theta_y}^2}}{\sqrt{(1+\sigma^2\omega_0^2)^2 \beta_4 + (1+\sigma^2\omega_0^2)(B_5+B_6)+B_7}}, \tag{17b}$$

$$B_4 = (k_{b\theta_y\theta_y}k_{bxx} - k_{bx\theta_y}^2)^2, \qquad B_5 = \omega_0^2 \gamma_I I_s k_{bxx}(k_{bxx}\gamma_I I_s \omega_0^2 + 2k_{bx\theta_y}^2 - 2k_{bxx}k_{b\theta_y\theta_y}), \tag{17c, d}$$

$$B_6 = \omega_0^2 \gamma_m m_s k_{b\theta_y\theta_y}(k_{b\theta_y\theta_y}\gamma_m m_s \omega_0^2 + 2k_{bx\theta_y}^2 - 2k_{bxx}k_{b\theta_y\theta_y}), \tag{17e}$$

$$B_7 = 2\omega_0^4 \gamma_m m_s \gamma_I I_s \{2k_{bxx}k_{b\theta_y\theta_y} - \omega_0^2(\gamma_I I_s k_{bxx} + \gamma_m m_s k_{b\theta_y\theta_y})\}$$
$$+\omega_0^4 \gamma_m m_s \gamma_I I_s \{\gamma_m m_s \gamma_I I_s \omega_0^4 - 2k_{bx\theta_y}(1-\sigma^2\omega_0^2)\}. \tag{17f}$$

Only the force transmissibility, as given as follows, is predicted by the simple model [14]. Compare it with equation (17a):

$$\hat{R}_{F_{xba},F_{xsa}}(\omega_0) = k_{bxx}\gamma_m \sqrt{(1+\sigma^2\omega_0^2)}/\sqrt{(k_{bxx}-\omega_0^2\gamma_m m_s)^2 + (k_{bxx}\omega\sigma)^2}. \tag{18}$$

Equations (17) and (18) are compared in Figure 7. Our model predicts higher $R_{F_{xba},F_{xsa}}(\omega_0)$ and ω_2 than the simple model due to the additional constraints imposed by $[K]_{bm}$. Also, it is clear that the simple model cannot predict dynamic moment transfer through the bearing. The bearing transmissibility functions $R(\omega_0)$ predicted by our model for three different axial preloads are shown in Figure 8. Note that the resonant amplitudes vary

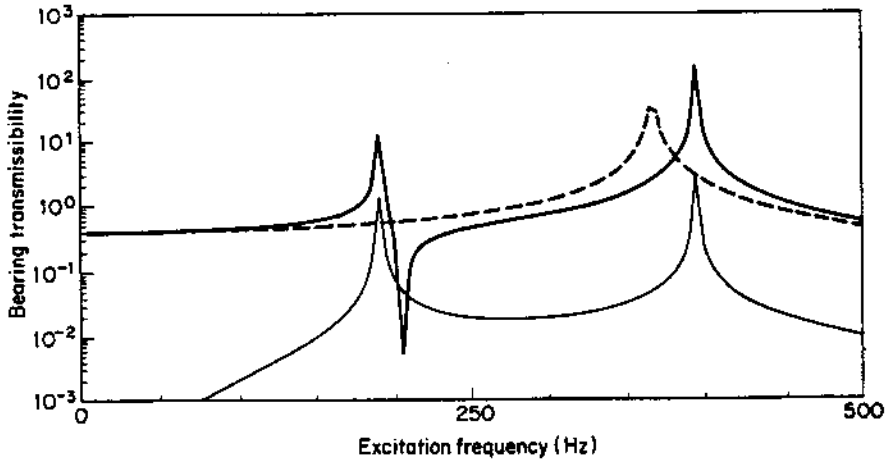

Figure 7. Bearing transmissibility spectra $R_{f_{wba},F_{xsa}}(\omega_0)$ for example case I. Here (——) R1 is force transmissibility with $f_{wba} = F_{xba}$ and (——) R2 is moment transmissibility with $f_{wba} = M_{yba}$, as predicted by our model with DOF = 2 and (- - -) the simple model by Kraus *et al.* [14] with DOF = 1.

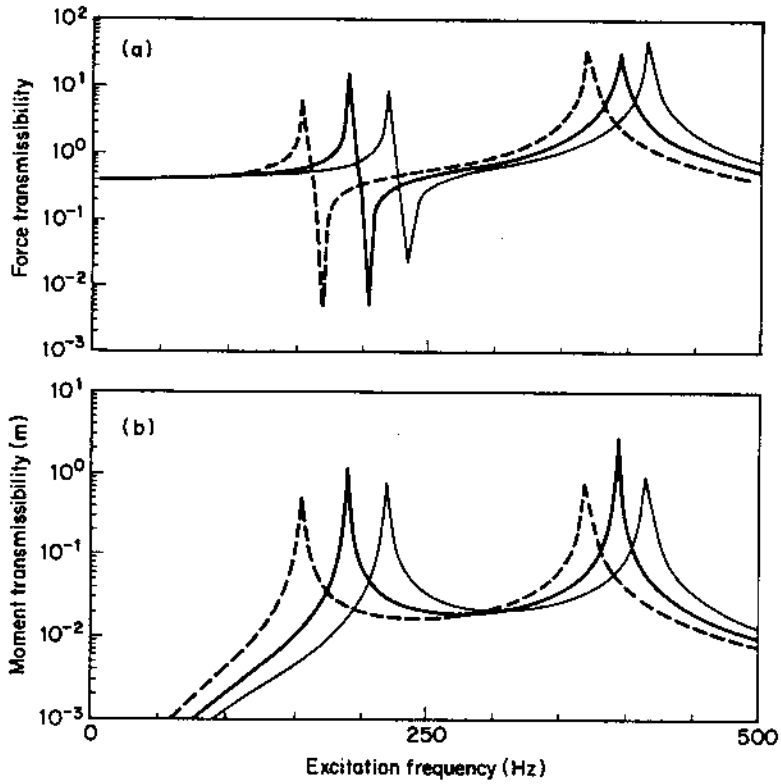

Figure 8. Effect of mean axial preload on the bearing transmissibility spectra $R_{f_{wba}F_{xba}}(\omega_0)$ defined by equation (17) for example case I. (a) Force transmissibility with $f_{wba} = F_{xba}$. (b) Moment transmissibility with $f_{wba} = M_{yba}$. Preload: - - -, 115 N; ——, 190 N; ——, 285 N.

depending on the amount of axial preload and the resonant frequencies increase with increasing preloads, as expected.

8. EXAMPLE CASE II: RIGID SHAFT AND PLATE SUPPORTED ON FLEXIBLE MOUNTS

8.1. VIBRATIONS MODELS

The physical system of example case I is modified to include flexible mounts, $[K]_v \neq [0]$, and mean radial shaft force $F_{rsm} \neq F_{rsm}(t)$ and $F_{rsa}(t) = F_{rsa1}\, e^{i\omega_0 t}$, as shown in Figure 9($a$). The bearing is also preloaded in the axial direction. This is modeled by using lumped parameter theory with finite mount stiffness coefficients $k_{vj}, j = x, y, z, \theta_x, \theta_y$ or θ_z, as illustrated in Figure 9(b). Since the rigid shaft assumption still holds, $F_{rsm} = F_{rbm}$ is applied directly on the bearing in a manner similar to the axial preload. The bearing matrix $[K]_{bm}$ in Figure 9(b) has non-negligible stiffness coefficients k_{bxx}, k_{byy}, k_{bzz}, $k_{b\theta_x\theta_x}$, $k_{b\theta_y\theta_y}$, $k_{bx\theta_y}$, $k_{by\theta_x}k_{bxz}$ and $k_{bz\theta_y}$, which are functions of the mean bearing load vector $\{f\}_{bm} = \{f\}_{sm}$ or the mean bearing displacement vector $\{q\}_{bm} = \{q\}_{sm} - \{q\}_{cm}$, as given by Part I [10]. Conversely, White [11] has investigated this problem using a simple model with two degrees of freedom as shown in Figure 9(c). It may be noted that his bearing system model did not include the effect of axial preload.

Like example case I, the governing equations (1) and (2) can be modified and reduced to four uncoupled sets of differential equations. The first two sets associated with $\theta_{ysa}(t)$ and $\theta_{zca}(t)$ are homogeneous. The third set is similar to equation (11) but with x and y subscripts interchanged, and two mount stiffness coefficients k_{vy} and $k_{v\theta_x}$ included. However, it is still homogeneous and therefore has only a trivial steady state solution. The final set corresponds to $\{q\}_a(t) = \{u_{xsa}(t), u_{zsa}(t), \theta_{ysa}(t), u_{xca}(t), u_{zca}(t), \theta_{yca}(t)\}^T$ with

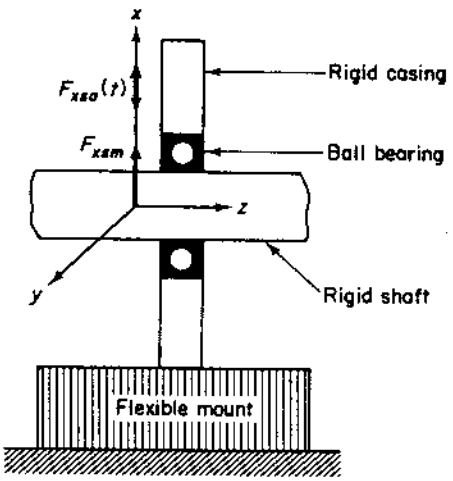

(a)

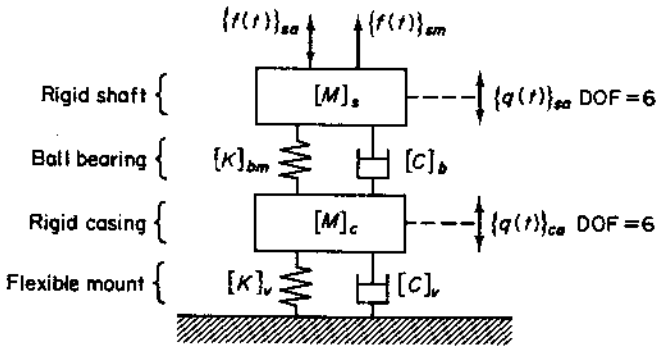

(b)

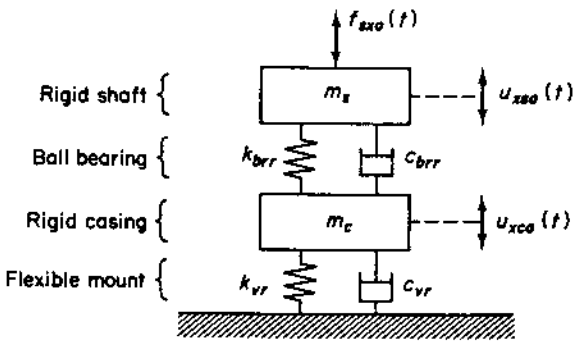

(c)

Figure 9. Example case II: rigid shaft, ball bearing and rigid plate system supported by flexible mounts and subjected to alternating radial force $F_{xso}(t)$ applied at the shaft. (a) Physical system; (b) proposed multi-degree-of-freedom vibration model with DOF = 12; (c) White's vibration model [11] with DOF = 2.

$[M]_s$, $[M]_c$, $[K]_{bm}$ and $[K]_v$ of equation (2) reduced to

$$[M]_s = \begin{bmatrix} m_s & 0 & 0 \\ 0 & m_s & 0 \\ 0 & 0 & I_s \end{bmatrix}, \qquad [M]_c = \begin{bmatrix} m_c & 0 & 0 \\ 0 & m_c & 0 \\ 0 & 0 & I_c \end{bmatrix}, \tag{19a, b}$$

$$[K]_{bm} = \begin{bmatrix} k_{bxx} & k_{bxz} & k_{bx\theta_y} \\ k_{bxz} & k_{bzz} & k_{bz\theta_y} \\ k_{bx\theta_y} & k_{bz\theta_y} & k_{b\theta_y\theta_y} \end{bmatrix}, \qquad [K]_v = \begin{bmatrix} k_{vx} & 0 & 0 \\ 0 & k_{vz} & 0 \\ 0 & 0 & k_{v\theta_y} \end{bmatrix}. \tag{19c, d}$$

The vibration model by White [11] may be formulated by retaining only two equations corresponding to $u_{xsa}(t)$ and $u_{xca}(t)$ and excluding all bearing and mount stiffness coefficients except for k_{bxx} and k_{vx}.

Analytical eigensolution of the undamped system is not possible since it requires solving for the zeroes of a sixth order polynomial in ω^2. Therefore, this problem was solved numerically by using an eigenvalue routine [19]. With the same system parameters as in example case I, with three different F_{xsm}, natural frequencies and modes were found as given in Table 5(b) and 5(c) for both our and White's models. Corresponding bearing mean loads $\{F_{xbm}, F_{zbm}, M_{ybm}\}^T$ and relevant bearing stiffness coefficients computed by using the method derived in Part I [10] are listed in Table 5(a). It is indicated in Tables 5(b) and 5(c) that only the first and fifth modes of our model are predicted by White's model; here the superscript $\hat{}$ is again used to denote estimation based on the simple model. The first natural frequency ω_1 predictions by both models are very similar. But

TABLE 5

Results of example case II†

(a) Computed bearing mean loads and stiffness coefficients

Shaft mean load, F_{xsm} (N)	Bearing loads‡		Bearing stiffness coefficients					
	F_{zbm} (N)	M_{ybm} (Nm)	k_{bxx} (N/m)	k_{bxz} (N/m)	$k_{bx\theta_y}$ (N)	k_{bzz} (N/m)	$k_{bz\theta_y}$ (N)	$k_{b\theta_y\theta_y}$ (Nm)
44	198	0·62	2·26E7	5·84E7	−2·90E5	8·50E7	−3·10E3	1·71E4
94	216	1·16	2·64E7	1·14E7	−2·33E5	8·55E7	−1·36E4	1·72E4
122	229	1·38	2·93E7	1·40E7	−1·98E5	8·60E7	−2·19E4	1·74E4

(b) Undamped natural frequencies (Hz)

Mean shaft load, F_{xbm} (N)	Proposed model (DOF = 6)						Simple model (DOF = 2)	
	ω_1	ω_2	ω_3	ω_4	ω_5	ω_6	$\hat{\omega}_1$	$\hat{\omega}_5$
44	93	100	111	287	350	607	97	321
94	96	100	115	300	351	614	97	345
122	97	100	117	308	364	620	98	362

(c) Modes of vibration§

Proposed model (DOF = 6)						Simple model (DOF = 2)	
$\{\phi\}_1$	$\{\phi\}_2$	$\{\phi\}_3$	$\{\phi\}_4$	$\{\phi\}_5$	$\{\phi\}_6$	$\{\hat{\phi}\}_1$	$\{\hat{\phi}\}_5$
0·217	0·031	−0·030	−0·130	0·180	0·044	0·218	0·229
−0·035	0·203	0·003	0·022	−0·036	0·236		
1·648	0·084	5·966	−0·354	−1·245	−0·068		
0·171	0·084	−0·071	0·107	−0·139	−0·031	0·187	−0·178
−0·027	0·194	0·008	−0·018	0·028	−0·165		
0·167	0·009	0·917	4·648	3·295	0·073		

† Other system parameters are $m_s = 10{\cdot}0$ kg, $I_s = 0{\cdot}025$ kgm^2, $m_c = 15{\cdot}0$ kg, $I_c = 0{\cdot}03$ kgm^2, $\sigma = 1$ E-6 s, $k_{vx} = 1$ E7 N/m, $k_{vz} = 1$E7 N/m, $k_{x\theta_y} = 1$ E5 Nm.

‡ $F_{xbm} = F_{xsm}$.

§ These are for mean shaft load $F_{xsm} = F_{xbm} = 94$ N.

the ω_5 prediction, the mode of which is similar to the second mode of example case I, indicates a few discrepancies. White's model also underestimates this natural frequency due to the incomplete bearing stiffness model employed. Here again our predicted modes include δ_{xa}, δ_{za} and β_{ya} displacements of shaft and casing components which are not considered by White's model.

8.2. FREQUENCY RESPONSE

The forced harmonic response solution was also determined numerically by using the dynamic stiffness approach outlined in section 6. Driving point (with $j = s$) and cross point (with $j = c$) accelerance spectra $A_{q_{wja}F_{xsa}}(\omega_0)$ are given in Figure 10 with $q_{wja} = u_{xja}$, u_{zja} or θ_{yja} for both models. Here, one can observe that White's [11] model overestimates the magnitudes of the accelerance and cannot predict, unlike our model, axial $u_{za}(t)$ and $\theta_{ya}(t)$ angular motions on the shaft and casing. The bearing transmissibility spectra $R_{f_{wba},F_{xsa}}(\omega_0)$ for $f_{wba} = F_{xba}$, F_{zxa} or M_{yba}, which indicate that transmissibilities corresponding to F_{zxa} and M_{yba} are not predicted by using White's model, as shown in Figure 11. Such loads also serve as mechanisms for vibration transmission through the bearing to the casing, in addition to F_{xba}. The mount transmissibility spectra $R_{f_{wba},F_{xsa}}(\omega_0)$ as shown in Figure 11 indicate that F_{zva} and M_{yva} are also transmitted to the mounts in addition to F_{xva} due to casing motions in x, z and θ_y directions. The effect of mean radial bearing force F_{xbm} on the load transmissibilities $R(\omega_0)$ through the bearing is shown in Figure 12 for three different mean loads. One can again observe that the resonant amplitudes and frequencies are mean load dependent through $[K]_{bm}$. Similar trends show that an increase in mean load raises the resonant frequencies although the effects are not as pronounced as those found in example case I.

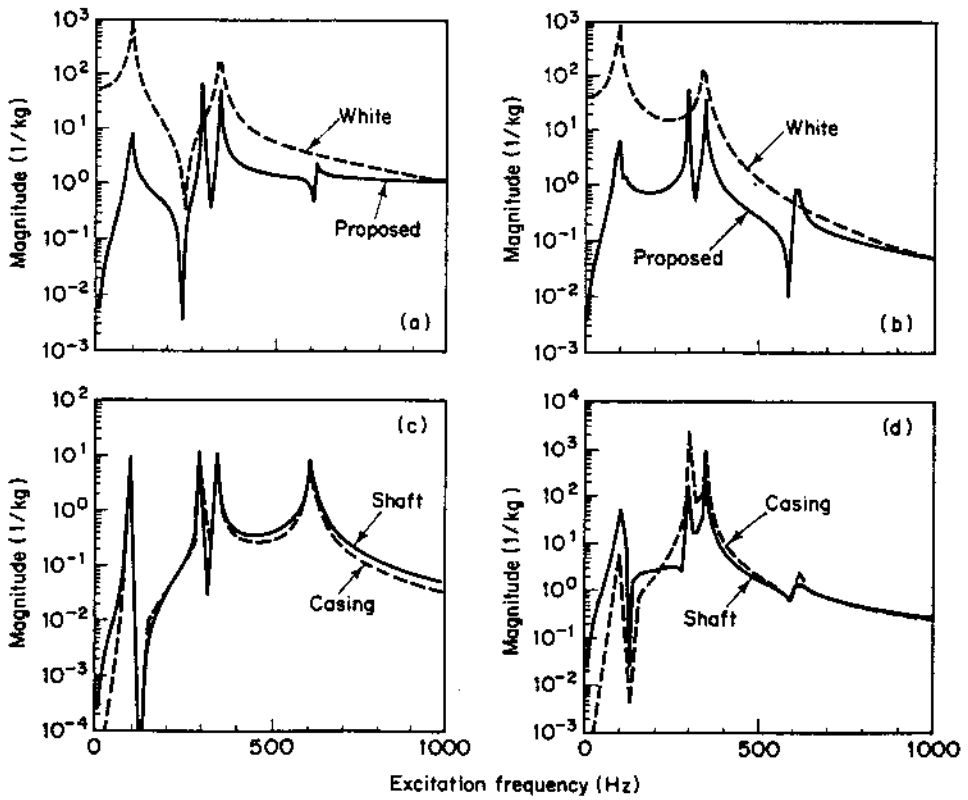

Figure 10. Accelerance spectra $A_{q_{wja},F_{xsa}}(\omega_0)$ for example case II as predicted by our formulation and White's model [11]. (a) Driving-point accelerance of shaft with $q_{wja} = u_{xsa}$; (b) cross-point acclerance of casing with $q_{wja} = u_{xca}$; (c) accelerance with $q_{wja} = u_{zsa}$ for shaft and $q_{wja} = u_{zca}$ for casing; (d) accelerance with $q_{wja} = \theta_{ysa}$ for shaft and $q_{wja} = \theta_{yca}$ for casing.

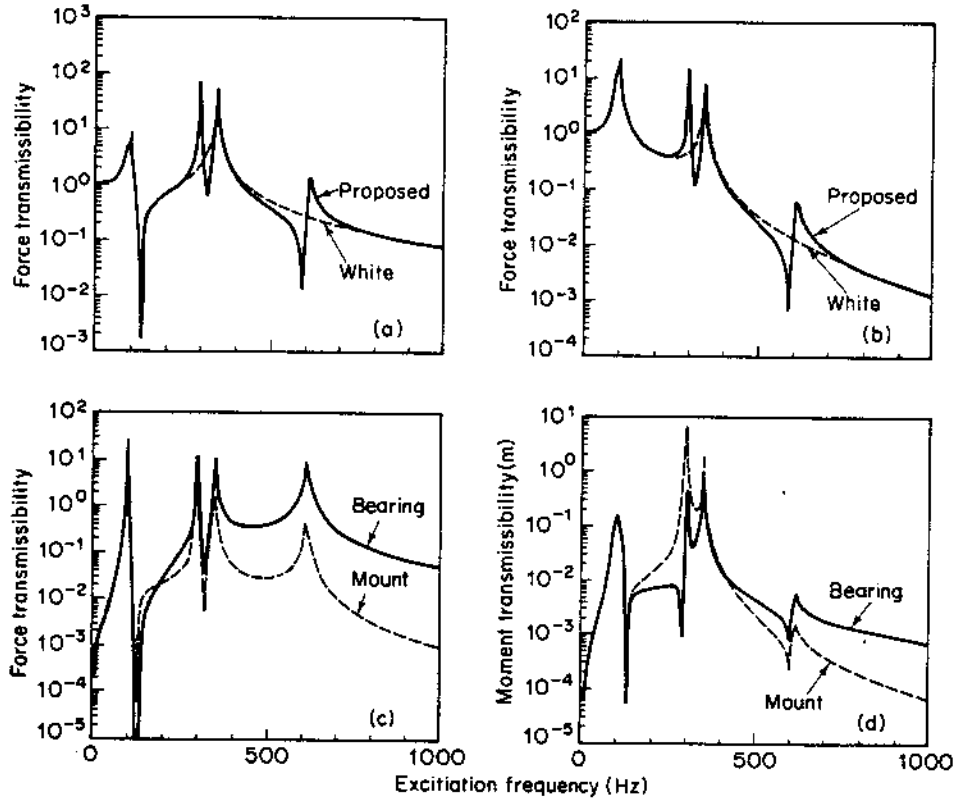

Figure 11. Bearing $R_{f_{wba}F_{xsa}}(\omega_0)$ and mount $R_{f_{wva}F_{xsa}}(\omega_0)$ transmissibility spectra for example case II as predicted by our formulation and White's model [11]. (a) Bearing force transmissibility with $f_{wba} = F_{xba}$; (b) mount force transmissibility with $f_{wva} = F_{xva}$; (c) force transmissibility with $f_{wba} = F_{zba}$ for bearing and $f_{wva} = F_{zva}$ for mount; (d) moment transmissibility with $f_{wba} = M_{yba}$ for bearing and $f_{wva} = M_{yva}$ for mount.

9. EXAMPLE CASE III: EXPERIMENTAL STUDY

9.1. PHYSICAL SET-UP

The final example case examines the experimental set-up of Lin [9] as shown in Figure 13(a). This system is similar to that of Figure 1 and consists of a 159 mm long × 25 mm diameter non-rotating shaft supported by two rolling element bearings of 25 mm bore × 51 mm outer diameter. One is supported on a rectangular plate of approximate dimensions 762 mm × 457 mm × 9 mm and the second is rigidly connected to the base. The plate is also bolted to a massive base structure. The excitation force F_{ys} consists of a mean $F_{ysm} = 445$ N via a preloaded spring and an alternating $F_{ysa}(t)$ component applied transversely at the free end of the shaft by using a vibrating shaker. Driving and cross-point accelerance spectra were measured at the shaft and on the plate respectively. Further details of this experiment are summarized in reference [9].

9.2. BEARING ANALYSIS

Initially, only the static analysis can be performed to obtain $[K]_{bm}$ for this experimental system by using the method proposed in Part I [10]. The static analysis neglects plate flexibility; this assumption is valid since the bearing mean loads are sufficiently low and do not deflect the plate. The shaft–bearing system is statically indeterminate, as shown in Figure 13(b). The mean force F_{ysm} on the shaft produces a mean bearing load vector $\{f\}_{bm} = \{0, F_{ybm}, F_{zbm}, M_{xbm}, 0\}^T$ which depends on the mean bearing displacement vector $\{q\}_{bm} = \{0, \delta_{ym}, \delta_{zm}, \beta_{xm}, 0\}^T$. The proposed bearing matrix $[K]_{bm}$ includes stiffness coefficients k_{bxx}, k_{byy}, k_{bzz}, $k_{b\theta_x\theta_x}$, $k_{b\theta_y\theta_y}$, $k_{bx\theta_y}$, $k_{by\theta_x}$, k_{byz} and $k_{bz\theta_x}$, which are direct functions of $\{q\}_{bm}$. In contrast, the conventional bearing models include only k_{bxx}, k_{byy} and k_{bzz}

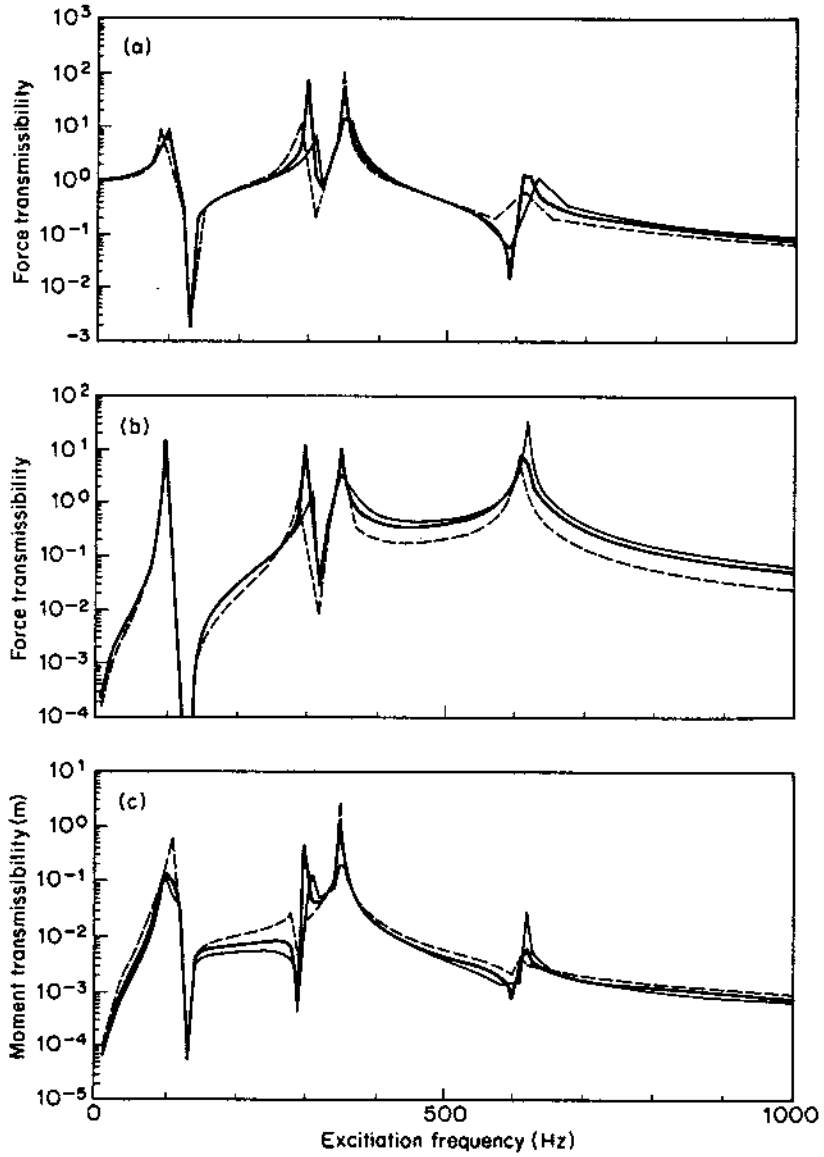

Figure 12. Effects of the mean radial bearing force F_{xbm} on the bearing transmissibility spectra $R_{f_{wba},F_{xsa}}(\omega_0)$ for example case II. (a) Force transmissibility with $f_{wba} = F_{xba}$; (b) force transmissibility with $f_{wba} = F_{zba}$; (c) moment transmissibility with $f_{wba} = M_{yba}$. Mean load: - - -, 44 N; ——, 94 N; ——, 122 N.

coefficients. From Figure 13(b), the force and moment equilibrium equations for this system are

$$F_{yb_1m} + F_{yb_2m} - F_{ysm} = 0, \tag{20a}$$

$$M_{yb_1m} + M_{yb_2m} - F_{yb_2m}l_1 + F_{ysm}(l_1 + l_2) = 0, \qquad F_{zb_1m} + F_{zb_2m} = 0. \tag{20b, c}$$

Since the shaft-bearing system is statically indeterminate, bending theory for the shaft and rigid-body motion constraint in the z direction can be used to estimate stiffness coefficients:

$$EI\delta_{y_2m} - EI\delta_{y_1m} + F_{yb_1m}(l_1^3/6) + M_{yb_1m}(l_1^2/2) = 0, \tag{21a}$$

$$EI\beta_{x_2m} - EI\beta_{x_1m} + F_{yb_1m}(l_1^2/2) + M_{yb_1m}l_1 = 0, \qquad \delta_{z_1m} - \delta_{z_2m} = 0. \tag{21b, c}$$

Additionally, six non-linear algebraic equations defined by the mean bearing load-displacement relations as given in Part I are required. These non-linear algebraic equations have been solved by using the Newton-Raphson method [23, 24]. Since mean loads on each bearing are sufficiently large, the bearing stiffness coefficients for both bearings are almost identical, as listed in Table 6 along with other system parameters.

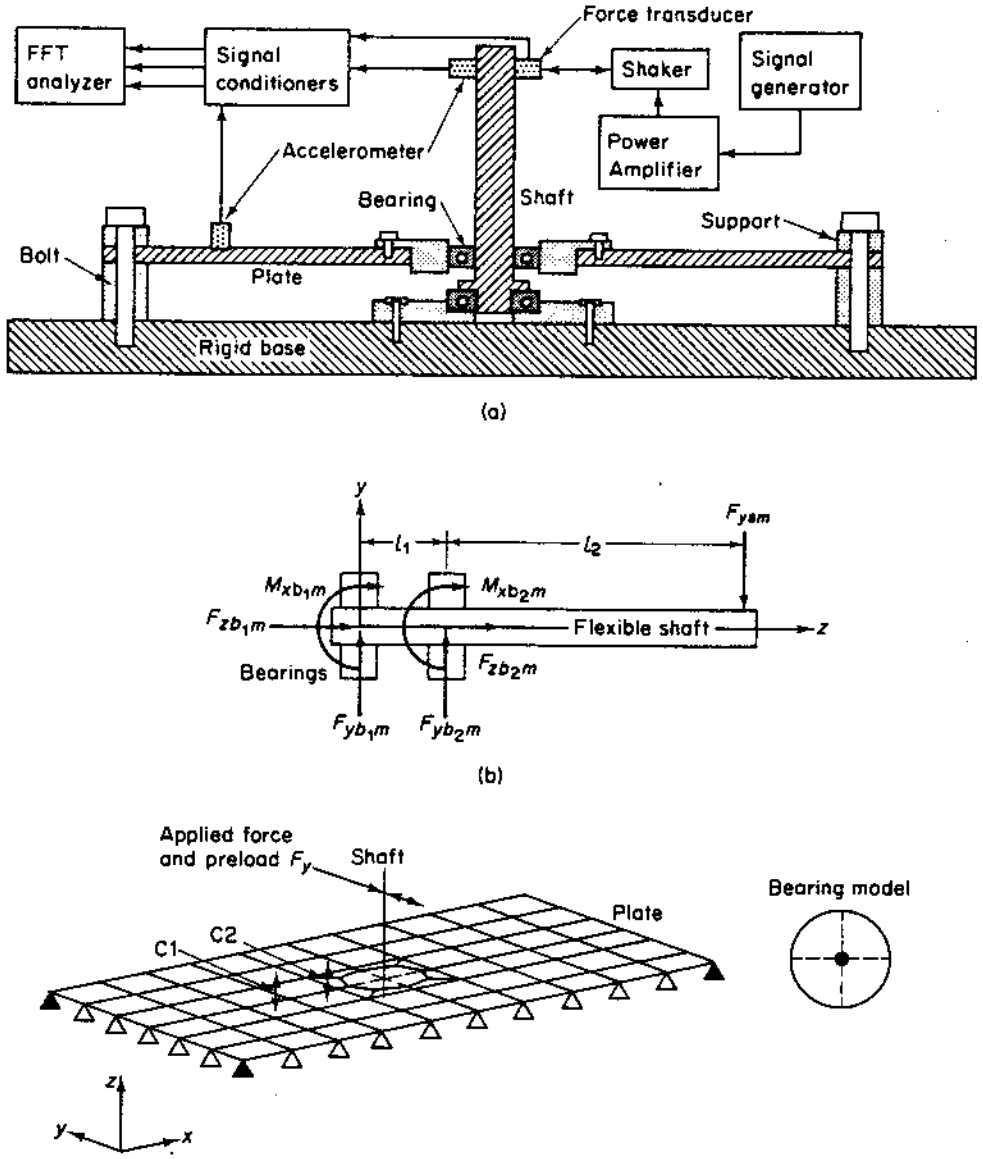

Figure 13. Example case III. (a) Schematic of the experimental set-up consisting of an overhung shaft, two ball bearings and a rectangular plate [9]; (b) static model of shaft and bearings used for computing $[K]_{bm}$; (c) finite element model of the experimental system shown in (a); the generalized stiffness matrix elements for the bearing model are shown by dashed lines, connecting one node on the shaft to four nodes on the plate; - - -, bearing stiffness element; △, simply supported; ▲, clamped; ↔, measured response.

TABLE 6

Design and estimated parameters for two identical rolling element bearings used in example case III

Load-deflection exponent, $n = 3/2$	A_0† = 0·05 mm	k_{bzz} = 1·72E8 N/m
Load-deflection constant, K_n = 6·92E9 N/m^n	l_1 = 41 mm	$k_{bx\theta_y}$ = −2·56E5 N
Number of rolling element, $Z = 10$	l_2 = 84 mm	$k_{by\theta_x}$ = 3·52E5 N
Radial clearance, r_L = 5·0 E-5 mm	k_{bxx} = 1·44E8 N/m	$k_{bz\theta_x}$ = 4·02E5 N
Pitch diameter = 38.1 mm	k_{byy} = 3·69E8 N/m	$k_{b\theta_x\theta_x}$ = 4·19E4 Nm
Unloaded contact angle, $\alpha_0 = 0°$	k_{byz} = 2·04E8 N/m	$k_{b\theta_y\theta_y}$ = 1·02E4 Nm

† Unloaded distance between inner and outer raceway groove curvature centers.

9.3. SYSTEM STUDY

The proposed rolling element bearing stiffness matrix $[K]_{bm}$ is incorporated in a finite element model which includes shaft and plate dynamics, by using the formulation given in section 4.2. The finite element model shown in Figure 13(c) was implemented using commercial software [16]. The shaft component was modeled by using two-noded Timoshenko beam elements with axial degrees of freedom in addition to the bending motion. The plate model was constructed by using four-noded quadrilateral plate elements with shear deformation and rotary inertia effects. Each node has three translational and three rotational degrees of freedom. Four generalized stiffness matrices corresponding to the first bearing, each matrix being equivalent to $(1/4)[K]_{bm}$, are used to couple the single shaft node to four plate nodes. The second bearing connects one end of the shaft to a grounded node. The boundary conditions for the plate along the perimeter are chosen to be a combination of ideal clamps, $u_{xa}(t) = u_{ya}(t) = u_{za}(t) = \theta_{xa}(t) = \theta_{ya}(t) = \theta_{za}(t) = 0$, and simple supports $u_{za}(t) = 0$ as shown in Figure 13(c) in order to represent the physical model as closely as possible. Here, the energy dissipation is assumed to be given by the modal damping ratio $\zeta = 0{\cdot}03$. A sinusoidal force $F_{ysa}(t) = F_{ysa1}\, e^{i\omega_0 t}$ is applied at one end of the shaft to simulate the experiment.

Over the frequency range of 400 Hz to 2000 Hz, the driving point accelerance spectra $A_{u_{ysa},F_{ysa}}(\omega_0) = \ddot{u}_{ysa}/F_{ysa}$ are compared in Figure 14. The simple theory shown here represents the conventional way of modeling bearings, while other the features are exactly the same as in proposed model. Our predictions match measured spectra very well. Conversely, the simple model predicts slightly higher accelerance amplitude and lower resonant frequency in the vicinity of 800 Hz due to the incomplete bearing model used. Cross-point accelerance spectra $A_{u_{zca},F_{ysa}}(\omega_0) = \ddot{u}_{zca}/F_{ysa}$ are shown in Figures 15(a) and 15(b), where $\ddot{u}_{zca}$ is measured for two different locations on the plate as shown in Figure 13(c), and the excitation $F_{ysa}(t)$ is once again applied transversely at the shaft. Here, each predicted accelerance spectrum has been averaged over four points in the immediate vicinity of the measured location. Reasonable comparisons between the proposed model and experiment are seen. Here, the discrepancies are primarily due to physical set-up complexities and the limitations associated with the finite element model in describing some of these. In Figure 15, the simple model is not included because it predicts exactly

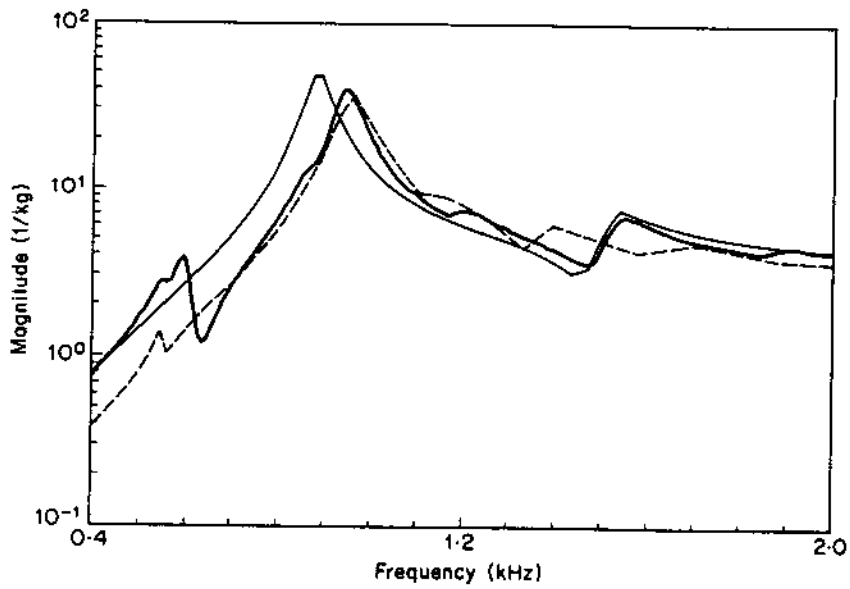

Figure 14. Driving-point accelerance spectra $A_{u_{ysa},F_{ysa}}(\omega_0)$ yielded by the proposed model (——), simple model (——) and experiment (- - -) for example case III.

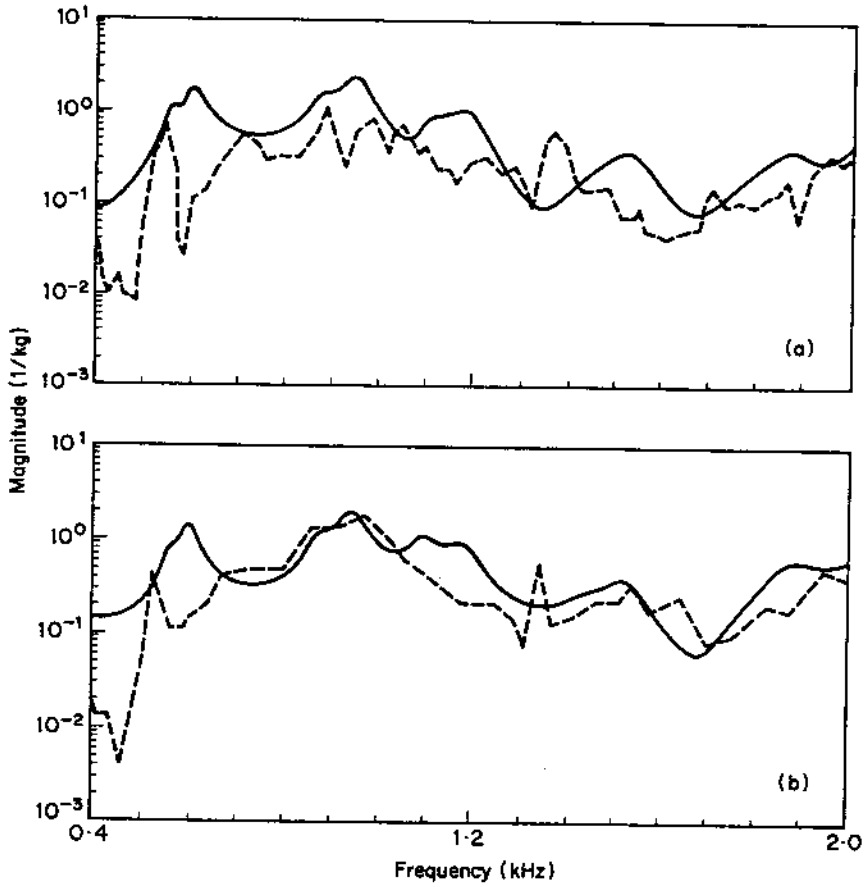

Figure 15. Cross-point accelerance spectra $A_{\ddot{u}_{zca},F_{xsa}}(\omega_0)$ yielded by the proposed model (——) and experiment (- - -) for example case III. In this case, the simple model predicts zero response $\ddot{u}_{zca}$ at the plate. (a) Point C1 (see Figure 13c); (b) point C2 (see Figure 13c).

zero out-of-plane or flexural motion of the plate. Next, the cross-point mobility level L_V is defined by averaging mean square mobility spatially over the entire plate and over a frequency bandwidth $\Delta\omega$. This level is directly related to the structure-borne noise or vibratory energy transmitted through the bearing;

$$L_V = 10 \log_{10} \{\langle V_{zca}^2 \rangle\}$$

$$= 10 \log_{10} \left\{ \frac{1}{2S_c \Delta\omega} \sum_{\Delta\omega} \sum_{S_c} \mathrm{Re} \left(\frac{\dot{u}_{zca} \dot{u}_{zca}^*}{F_{xsa} F_{xsa}^*} \right) \right\}, \qquad \mathrm{dB\ re} \langle V^2 \rangle_{\mathrm{ref}} = 1{\cdot}0 m^2/N^2 s^2, \tag{22}$$

TABLE 7

Predicted and measured cross-point mobility level L_V as defined by equation (22)

1/3 Octave band center frequency (Hz)	Experiment (dB)	Proposed model (dB)	Simple model (dB)
400	−102	−105	−∞
500	−92	−96	−∞
630	−95	−94	−∞
800	−88	−97	−∞
1000	−87	−95	−∞
1250	−97	−108	−∞
1600	−108	−115	−∞
2000	−106	−107	−∞

where ( )* implies the complex conjugate, S_c is the plate surface area and Re { } implies the real part of the complex number. Predictions of L_V by the proposed and the simple models are compared with experimental data in Table 7. It can be seen from this table that the proposed model predicts the experiment quite well and the simple model fails to predict any plate vibration. We can therefore conclude that our model is indeed valid for vibration transmission analyses.

10. CONCLUDING REMARKS

A new mathematical model for precision rolling element bearing has been developed and incorporated in linear system dynamic models, with use of lumped parameter and finite element modeling techniques, for vibration transmission studies of a generic single shaft–bearing–plate system. Stability studies indicate that the bearing system is dynamically stable for most of the practical designs. Through three example cases, including one experimental study, we have shown that our proposed vibration model is clearly superior to the models currently available in the literature. The current models tend to underestimate the resonant frequencies and force/moment transmissibilities, and overestimate the accelerance amplitudes as compared to our models. The proposed model also predicts how the vibratory bending motion on the shaft is transmitted to the casing illustrated through coupling coefficients of the proposed bearing stiffness matrix $[K]_{bm}$. Finally, the forced response trends indicated that an increase in the mean bearing loads increases system resonant frequencies. We are extending this model to predict vibration transmission in rotating equipment with multiple shafts, bearings and gears. Other applications are evident, as our theory is general in nature. However, it is restricted to linear systems. Bearing non-linearities are being examined in a parallel study.

ACKNOWLEDGMENTS

We wish to thank the NASA Lewis Research Center for supporting this research, and J. S. Lin and D. R. Houser for providing the experimental data of example case III.

REFERENCES

1. H. N. OZGUVEN 1984 *Journal of Vibration, Acoustics, Stress, and Reliability in Design, Transactions of the American Society of Mechanical Engineers* **106**, 59–61. On the critical speed of continuous shaft–disk systems.
2. A. D. DIMAROGONAS and S. A. PAIPETIS 1983 *Analytical Methods in Rotor Dynamics.* London: Applied Science.
3. J. S. RAO 1983 *Rotor Dynamics.* New York: John Wiley.
4. E. S. ZORZI and H. D. NELSON 1977 *Journal of Engineering for Power, Transactions of the American Society of Mechanical Engineers* **99**(1), 71–77. Finite element simulation of rotor-bearing systems with internal damping.
5. E. P. GARGIULO 1980 *Machine Design* **52**, 107–110. A simple way to estimate bearing stiffness.
6. A. KAHRAMAN, H. N. OZGUVEN, D. R. HOUSER and J. J. ZAKRAJSEK 1989 *Proceedings of the International Power Transmission and Gearing Conference, Chicago,* 375–382. Dynamic analysis of geared rotors by finite elements.
7. K. ISHIDA, T. MATSUDA and M. FUKUI 1981 *Proceedings of the International Symposium on Gearing and Power Transmissions, Tokyo,* 13–18. Effect of gearbox on noise reduction of geared device.
8. A. M. MITCHELL, F. B. OSWALD and H. H. COE 1986 *NASA Technical Report* 2626. Testing of UH-60A helicopter transmission in NASA Lewis 2240kW(3000-hp) facility.
9. J. S. LIN 1989 *M.S. Thesis, The Ohio State University.* Experimental analysis of dynamic force transmissibility through bearings.

10. T. C. LIM and R. SINGH 1990 *Journal of Sound and Vibration* **139**(2), 179–199. Vibration transmission through rolling element bearings, part I: bearing stiffness formulation.
11. M. F. WHITE 1979 *Journal of Applied Mechanics* **46**, 677–684. Rolling element bearing vibration transfer characteristics: effect of stiffness.
12. M. D. RAJAB 1982 *Ph.D. Dissertation, The Ohio State University.* Modeling of the transmissibility through rolling element bearing under radial and moment loads.
13. D. R. HOUSER, G. L. KINZEL, W. B. YOUNG and M. D. RAJAB 1989 *Proceedings of the Seventh International Modal Analysis Conference, Las Vegas,* 147–153. Force transmissibility through rolling contact bearings.
14. J. KRAUS, J. J. BLECH and S. G. BRAUN 1987 *Journal of Vibration, Acoustics, Stress, and Reliability in Design, Transactions of the American Society of Mechanical Engineers* **109**, 235–240. *In situ* determination of rolling bearing stiffness and damping by modal analysis.
15. STRUCTURAL DYNAMICS RESEARCH CORPORATION 1986 *SYSTAN User's Guide.* Milford, Ohio: Structural Dynamics Research Corporation.
16. G. J. DESALVO and J. A. SWANSON 1983 *ANSYS User's Manual.* Houston, Pennsylvania: Swanson Analysis System.
17. W. T. THOMPSON 1981 *Theory of Vibration with Applications.* Englewood Cliffs, New Jersey: Prentice-Hall.
18. W. D. PILKEY and P. Y. CHANG 1978 *Modern Formulas for Statics and Dynamics.* New York: McGraw-Hill.
19. L. MEIROVITCH 1980 *Computational Methods in Structural Dynamics.* Alphen aan den Rijn: Sijthoff & Noordhoff.
20. S. TIMOSHENKO, D. H. YOUNG and W. WEAVER, JR. (1974) *Vibration Problems in Engineering.* New York: John Wiley.
21. D. J. INMAN 1989 *Vibration with Control, Measurement, and Stability.* Englewood Cliffs, New Jersey: Prentice-Hall.
22. L. MEIROVITCH 1970 *Methods of Analytical Dynamics.* New York: McGraw Hill.
23. W. H. PRESS, B. P. FLANNERY, S. A. TEUKOLSKY and W. T. VETTERLING 1986 *Numerical Recipes.* Cambridge: Cambridge University Press.
24. J. ORTEGA and W. RHEINBOLDT 1970 *Iterative Solution of Nonlinear Equations in Several Variables.* New York: Academic Press.

APPENDIX: LIST OF SYMBOLS

$A(\omega)$	accelerance transfer function
A_0	unloaded distance between the inner and outer raceway groove curvature centers
$[C]$	system damping matrix
$[C]_b$	bearing damping matrix
DOF	degree of freedom
EI	flexural rigidity of the shaft
$F_{jba}(t)$	alternating bearing force in the $j = x, y, z$ or r direction
F_{jbm}	mean bearing force in the $j = x, y, z$ or r direction
$F_{jsa}(t)$	applied alternating force on the shaft, $j = x, y, z$ or r
F_{jsap}	complex Fourier coefficient of $F_{jsa}(t)$, $p = 1, 2, 3, \ldots$
F_{jsm}	applied mean force on the shaft, $j = x, y, z$ or r
$\{f(t)\}_a$	generalized alternating applied load vector
$\{f\}_{ap}$	complex Fourier coefficient of $\{f(t)\}_a$, $p = 1, 2, 3, \ldots$
$\{f\}_{bm}$	mean bearing load vector
$\{f(t)\}_{ca}$	alternating casing load vector
$\{f(t)\}_s$	total shaft load vector
$\{f(t)\}_{sa}$	alternating shaft load vector
$\{f\}_{sm}$	mean shaft load vector
I_c	mass moment of inertia of the casing
I_s	mass moment of inertia of the shaft
l_1, l_2	shaft lengths (see Figure 13(b))
K_n	rolling element load-deflection stiffness constant
$[K]$	system stiffness matrix
$[K]_{bm}$	proposed bearing stiffness matrix of dimension 6
$[K]_{bms}$	a matrix of dimension five as a subset of $[K]_{bm}$ with last row and column excluded

$[K]_v$ mount stiffness matrix
k_{vj} mount stiffness coefficient , $j = x, y, z, \theta_x, \theta_y, \theta_z$
k_{bwj} bearing stiffness coefficient, $w, j = x, y, z, \theta_x, \theta_y, \theta_z$
L_V spatially and frequency bandwidth averaged mean square mobility level (dB $re\ \langle V^2 \rangle_{ref} = 1{\cdot}0\ m^2/N^2s^2$)
$[M]$ system mass matrix
$[M]_s$ shaft mass matrix
$[M]_c$ casing mass matrix
M_{jba} alternating bearing moment about $j = x$ or y direction
M_{pbm} mean bearing moment about $p = x$ or y direction
m_s shaft mass
m_c casing mass
n rolling element load-deflection exponent
$\{q(t)\}_a$ generalized alternating displacement vector
$\{q\}_{ap}$ complex Fourier coefficient of $\{q(t)\}_a$, $p = 1, 2, 3, \ldots$
$\{q\}_{bm}$ mean bearing displacement vector
$\{q(t)\}_{ca}$ alternating casing displacement vector
$\{q(t)\}_{sa}$ alternating shaft displacement vector
$\{q\}_{sm}$ mean shaft displacement vector
$R(\omega)$ force or moment transmissibility transfer function
Re real part of a complex number
r_L bearing radial clearance
S_c total surface area of the casing plate in example case III
$[T]_b$ bearing field transfer matrix
$T_{jsa}(t)$ applied alternating torque on the shaft, $j = x, y$ or z
T_{jsm} applied mean torque on the shaft, $j = x, y$ or z
t time
$u_{jca}(t)$ alternating casing translational displacement in the $j = x, y$ or z direction
$u_{jsa}(t)$ alternating shaft translational displacement in the $j = x, y$ or z direction
$V(\omega)$ mobility transfer function
$\langle V^2 \rangle$ spatially and frequency bandwidth averaged mean square mobility
Z total number of rolling element
α_0 unloaded bearing contact angle
β_{pa} alternating bearing angular displacement about the $p = x$ or y direction
β_{pm} mean bearing angular displacement about the $p = x$ or y direction
$\Delta\omega$ frequency bandwidth
δ_{ja} alternating bearing translational displacement in the $j = x, y$ or z direction
δ_{jm} mean bearing translational displacement in the $j = x, y$ or z direction
Φ_j stability functions given by equation (6) and Table 1
$\{\phi\}_j$ mode shape vector corresponding to the jth natural frequency
$\{\mu\}_p$ complex Fourier coefficient of the principal co-ordinate vector, $p = 1, 2, 3, \ldots$
$\theta_{jca}(t)$ alternating casing angular displacement about the $j = x, y$ or z co-ordinate
$\theta_{jsa}(t)$ alternating shaft angular displacement about the $j = x, y$ or z co-ordinate
σ Rayleigh damping matrix proportionality constant
Ω_z mean rotational speed of the shaft
ω_j undamped natural frequency, $j = 1, 2, 3, \ldots$
ω_{jd} damped natural frequency, $j = 1, 2, 3, \ldots$
ω_0 fundamental frequency
ω_p excitation frequency, $p = 1, 2, 3, \ldots$
ζ_j modal damping ratio
$[\ ]^T$ transpose of a matrix or vector
$|\ |$ magnitude or determinant
$\dot{(\ )}$ first time derivative
$\ddot{(\ )}$ second time derivative
$(\ )^*$ complex conjugate
$\hat{(\ )}$ estimation based on simple models